

## Article

# Frequency Stability of AC/DC Interconnected Power Systems with Wind Energy Using Arithmetic Optimization Algorithm-Based Fuzzy-PID Controller

Ahmed H. A. Elkasem<sup>1</sup>, Mohamed Khamies<sup>1</sup>, Gaber Magdy<sup>2</sup> , Ibrahim B. M. Taha<sup>3,\*</sup> and Salah Kamel<sup>1,\*</sup> 

<sup>1</sup> Electrical Engineering Department, Faculty of Engineering, Aswan University, Aswan 81542, Egypt; ahmedhamdykasem2016@yahoo.com (A.H.A.E.); mohamedahmedmak@yahoo.com (M.K.)

<sup>2</sup> Department of Electrical Engineering, Faculty of Energy Engineering, Aswan University, Aswan 81528, Egypt; gabermagdy@aswu.edu.eg

<sup>3</sup> Department of Electrical Engineering, College of Engineering, Taif University, Taif 21944, Saudi Arabia

\* Correspondence: i.taha@tu.edu.sa (I.B.M.T.); skamel@aswu.edu.eg (S.K.)

**Abstract:** This article proposes an intelligent control strategy to enhance the frequency dynamic performance of interconnected multi-source power systems composing of thermal, hydro, and gas power plants and the high penetration level of wind energy. The proposed control strategy is based on a combination of fuzzy logic control with a proportional-integral-derivative (PID) controller to overcome the PID limitations during abnormal conditions. Moreover, a newly adopted optimization technique namely Arithmetic optimization algorithm (AOA) is proposed to fine-tune the proposed fuzzy-PID controller to overcome the disadvantages of conventional and heuristic optimization techniques (i.e., long time in estimating controller parameters–slow convergence curves). Furthermore, the effect of the high voltage direct current link is taken into account in the studied interconnected power system to eliminate the AC transmission disadvantages (i.e., frequent tripping during oscillations in large power systems–high level of fault current). The dynamic performance analysis confirms the superiority of the proposed fuzzy-PID controller based on the AOA compared to the fuzzy-PID controller based on a hybrid local unimodal sampling and teaching learning-based optimization (TLBO) in terms of minimum objective function value and overshoots and undershoots oscillation measurement. Also, the AOA's proficiency has been verified over several other powerful optimization techniques; differential evolution, TLBO using the PID controller. Moreover, the simulation results ensure the effectiveness and robustness of the proposed fuzzy-PID controller using the AOA in achieving better performance under several contingencies; different load variations, the high penetration level of the wind power, and system uncertainties compared to other literature controllers adjusting by various optimization techniques.

**Keywords:** load frequency control (LFC); multi-source power system; fuzzy logic control (FLC); high wind energy penetration



**Citation:** Elkasem, A.H.A.; Khamies, M.; Magdy, G.; Taha, I.B.M.; Kamel, S. Frequency Stability of AC/DC Interconnected Power Systems with Wind Energy Using Arithmetic Optimization Algorithm-Based Fuzzy-PID Controller. *Sustainability* **2021**, *13*, 12095. <https://doi.org/10.3390/su132112095>

Academic Editors: Nicu Bizon, Mamadou Baïlo Camara and Bhargav Appasani

Received: 18 September 2021

Accepted: 28 October 2021

Published: 2 November 2021

**Publisher's Note:** MDPI stays neutral with regard to jurisdictional claims in published maps and institutional affiliations.



**Copyright:** © 2021 by the authors. Licensee MDPI, Basel, Switzerland. This article is an open access article distributed under the terms and conditions of the Creative Commons Attribution (CC BY) license (<https://creativecommons.org/licenses/by/4.0/>).

## 1. Introduction

Consistent with the noticeable increase in energy demand, it is necessary to establish new energy sources. However, most efforts concern with establishing renewable energy sources (RESs) instead of conventional energy sources (CESs) due to the negative and harmful effects (e.g., global warming) of CES on our community [1–3]. So, energy planners and researchers make great efforts and strive to establish RESs paralleling with electrical networks for reducing CESs' hazards. In addition, RESs are clean and safe energy which be friendly to the environment [4]. While the establishment of RESs decreases the system inertia and may negatively affect the system stability [5,6]. Based on the aforementioned observations, the modern power grids will face a great challenge in keeping the system's frequency and the tie-line power stable. Therefore, it is important to keep the system stable

during these previous conditions, this occurs by applying load frequency control (LFC) to maintain the frequency and tie-line power of the system at their specified values [7]. In this regard, numerous control techniques/strategies have been conducted to make progress in modern power system frequency stability.

One of these strategies is optimal control, which includes linear quadratic regulators that are applied to regulate the frequency of two-area power systems considering AC/DC tie-lines [8]. Also in [9], the linear quadratic regulator is applied to enhance the frequency of the two-area power system in the presence of electrical vehicles. Another strategy known as robust control techniques, such as the second-order sliding mode controller, has been applied to regulate the frequency in multi-area power systems [10]. In [11], one robust control technique known as the  $\mu$ -synthesis approach is applied to regulate the frequency of the islanded micro-grid frequency containing (diesel engine generator, fuel cell, wind turbine, and PV array). In [12],  $\mu$ -synthesis approach has been applied to recover the frequency fluctuations under uncertainty weighing selection in power plants.  $H_\infty$  Controller has been designed in [13] to regulate the frequency of the power system while accounting for uncertainties. There is another type of these strategies known as model predictive control, which has been applied to enhance the performance of three-area interconnected power system considering the penetration of wind turbines [14]. Also, there are intelligent control strategies such as (e.g., artificial neural network and fuzzy logic control (FLC)) have been applied to counteract the system's frequency deviations during disturbances in the presence of tidal power units, electrical vehicles, energy storage systems, and solar power systems [15,16] and so on. While all these strategies were successful in resolving LFC difficulties, they depended on the designer's knowledge and experience, experimenting, and trial and error procedures in finding controller parameters, and it takes a very long time to approximate their parameters.

On the other hand, the proportional-integral-derivative (PID) controller and its forms are still the most popular controller due to their good characteristics such as simplicity and low cost [17]. However, the PID controllers are sensitive to system parameter variations (i.e., system uncertainties) and nonlinearities [18]. Thus, the FLC strategy has been proposed to support the PID controller performance in enhancing the dynamic frequency stability of modern power systems. The main advantages of the fuzzy controller include its simplicity of execution, high sensitivity to system fluctuations, and the ability to safely handle changes in the operating point or system parameters due to online updating of the controller parameters [19]. The first attempt in using the FLC for solving the LFC problem with the PID controller was conducted in [20]. Additionally, the self-tuning Fuzzy-PID controller was proposed to enhance the frequency stability of the interconnected power system, consisting of two areas [21]. Also, the fuzzy-PID controller has been utilized to stabilize the frequency of a multi-source power system [22]. Where the proposed Fuzzy-PID controller parameters have been selected based on an optimization technique. In addition, the Fuzzy-PID controller has been utilized to improve the stability of power system frequency considering the flexible AC transmission system devices (i.e., the static synchronous series compensator, the unified power flow controller, and the interline power flow controller) effect in [23,24]. The FLC is presented by parameters (i.e., inputs, scaling factors, membership functions, and rule base) that have not specific rules which can be followed to detect their values. Generally, trial and error methods have been used to select the parametric values, but these methods may not give the best performance. In this regard, this study proposes selecting the scaling factors of the fuzzy-PID controller based on a new meta-heuristic technique known as the Arithmetic Optimization Algorithm (AOA).

Therefore, there is another choice to take care of the LFC issue: to utilize various optimization methods and these are successfully utilized to manage the nonlinear functions associated with the LFC design. These several optimization techniques are applied for finding the optimal controller parameters to overcome the LFC problem and achieve more system security. The utilized techniques by researchers in the LFC issue such as; grasshopper optimization algorithm [25], ant colony optimization technique [26], Jaya

algorithm [27], particle swarm optimizer [28], firefly algorithm [29], hybrid pattern search shuffled-frog leaping algorithm [30], multi-objective genetic algorithm [31], grey wolf optimizer [32], sine cosine algorithm [33], harris hawks optimizer and salp swarm algorithm [34], lightning-attachment procedure optimization (LAPO) [35] and improved LAPO [36]. However, these techniques achieve exceptional performance by ensuring effectual LFC design. They have a slow convergence rate, restricted search capability, as well as local optimum convergence. On the other hand, the AOA algorithm has been made to overcome previous limitations related to different optimization techniques. The superiority of AOA than other conventional optimization algorithms returns to the gradient-free mechanism and its capability to avoid the local solutions and obtain the global solution with little search agents. Also, many experimental results show that, AOA provides very promising results in solving real-world engineering design. So, this study applied the AOA algorithm for fine-tuning the proposed fuzzy-PID controller parameters due to its promising results in solving several real-world engineering design problems [37]. Also, the AOA recently gave a distinguished performance in medicine field (i.e., evaluate images of COVID-19) [38].

The interconnected multi-source power systems need strong links (tie-lines) utilized in structural power exchange between different control areas. Also at abnormal conditions, these links provide a support to inter-area. Several studies have been maiden about the topic of LFC with the presence of AC transmission line only without HVDC line connection [39,40]. However, many problems related to the AC interconnection between areas in the power system, especially long-distance power transmission, remain. The problems associated with the AC interconnection can be mentioned as frequent tripping occurs at the instant of large power oscillations, an increase in fault current level, which leads to damage in the power system and transmission oscillations from one area to another, which causes deterioration in system dynamic performance. So this study proposes using of HVDC interconnection besides the AC tie line for transmitting the bulk power over the long distance to eliminate the demerits of the AC transmission lines and according to good features of HVDC transmission. The attractive features of HVDC links are summarized as: there are converters in HVDC lines that give the ability to fast controllability in power between interconnected areas. It can overcome the transient stability problems associated with AC transmission [41]. According to the point of obtaining stabilizing in the electrical power systems such as mentioned previously when adding HVDC lines, there are several studies deal with the issue of predicting processes of wind speed during participation in electrical power systems using different meta-heuristic techniques. These researchers seek to avoid fluctuations when wind speed exceeds the permissible limits [42–45]. On the other hand, there are off-shore wind turbines which characterized by a high average speed compared to on-shore wind turbines. Also, those off-shore wind turbines produce more electricity than on-shore wind turbines. Therefore, many researchers strive to choose the best site of off-shore wind turbines in coastal areas such as Turkey and USA to generate more electricity and link between these turbines and main electrical network to meet the need for citizens [46,47].

In terms of LFC issues, traditional controllers, such as the PID controller, have some challenges in parameter tuning and have not accommodated system stability in the face of uncertainties. Moreover, few studies applied fuzzy-PID controller to diminish the demerits of PID controller, but the parameters of the fuzzy-PID has been selected based in conventional and heuristic optimization algorithms. Furthermore, the renewables penetration effect has been considered in few studies, and not considered in other works [22,24,48]. Additionally, the effect of HVDC has been ignored in most works related to LFC studies [39,40]. So, this study proposes a robust control strategy based on Fuzzy-PID controller to keep the stability of systems involving different types of generating units in addition to renewable sources. In addition, the parameters of the fuzzy-PID controller have been selected based on a novel meta-heuristic algorithm known as AOA algorithm due to its merits. Unlike, previous works which have neglected the parameters variations effect [14,22],

the control design consider, system nonlinearities and system uncertainties have been considered during designing the proposed control strategy. Finally, the effect of HVDC has been considered to eliminate the demerits of AC transmission lines. Furthermore, Table 1 introduces a comparison between the motivation of this work and other studies.

**Table 1.** Comparison between this work and previous mentioned studies.

Properties	[25]	[39]	[40]	[49]	[50]	[50]	This Study
Type of controller	Fuzzy-PID controller	Optimal PI-PD cascaded controller	Optimal PID controller	Optimal PID controller	Optimal PID controller	Fuzzy-PID controller	Fuzzy-PID controller
Adoption of controller design on	Grasshopper optimization algorithm (GOA)	Flower pollination algorithm (FPA)	Grey wolf optimization (GWO)	Differential evolution (DE)	Teaching-learning based optimization (TLBO)	Hybrid local unimodal sampling (LUS) with TLBO	Arithmetic optimization algorithm (AOA)
Penetration of renewable energy sources	Not considered	Not considered	Not considered	Not considered	Not considered	Not considered	Considered with high penetration of wind energy
Effect of system uncertainties	considered	Not considered	considered	Not considered	Not considered	Not considered	considered
Effect of HVDC link	Not considered	Not considered	Not considered	considered	considered	considered	considered

The main contribution of this study can be summarized as follows:

- i. Proposing a fuzzy-PID controller for stabilizing the frequency of interconnected multi-source power systems considering high wind power penetration.
- ii. The proposed controller parameters have been selected via a new meta-heuristic optimization technique known as AOA algorithm according to its noteworthy features. While, it is the first attempt to apply the AOA algorithm in adjusting and optimizing the frequency controller parameters, thus enhancing the stability of the power system.
- iii. Considering, the effect of HVDC links to eliminate the problems related to the AC links.
- iv. Considering load disturbance, renewable power penetration (i.e., wind power), and system parameters variations during designing the parameters of the proposed fuzzy-PID controller-based AOA algorithm.
- v. Comparing the performance of the AOA algorithm with other optimization algorithms such as differential evolution (DE) and teaching-learning based optimization (TLBO) for selecting the parameters of the PID controller in hybrid two-area power system.
- vi. Comparing the performance of the proposed control strategy with other techniques performances such as; PID controller-based differential evolution (PID-DE) [49], PID controller-based teaching-learning based optimization (PID-TLBO) [50], and fuzzy-PID controller-based a hybrid local unimodal sampling (LUS) with TLBO (Fuzzy-PID-LUS-TLBO) [50] in order to ensure the effectiveness and robustness of the proposed controller.

The remainder of this research is summarized as follows: the modeling and configuration of the studied interconnected power system considering wind energy are discussed in Section 2. Section 3 presents the proposed fuzzy-PID controller methodology, the proposed optimization technique AOA, and the construction of the proposed control strategy. Then, Section 4 presents the simulations and investigation results. Finally, the conclusion of this work is mentioned in Section 5.

## 2. Modeling and Configuration of the Studied System

### 2.1. A dynamic Model of Two-Area Interconnected Power System

This article discusses the LFC issue of interconnected multi-source power systems. Where the studied system is composite of two-areas which interconnected together by a tie-line. Three power plants (i.e., the reheat thermal unit, the gas unit and the hydro unit) are included in each area of the investigated power system. Moreover, each unit in both areas has its speed governing system, turbine, and generator. The capacity or rating power of the investigated system is 2000 MW [51]. Also, the system dynamic performance has been investigated in the presence and absence of an HVDC link. The fuzzy-PID controller is proposed to be equipped in both areas for each generation unit to minimize the oscillations in both area frequencies and tie-line power between them. The input signals of the proposed fuzzy-PID controller represent the area control error (ACE) and its derivative, while the output signal represents the secondary control action on each generated unit. Figure 1 shows the dynamic model of the studied two-area interconnected power system and the schematic diagram is shown in Figure 2. The nominal parameters' values of the studied power system are given in Table 2. The ACEs in both areas can be obtained according to formulas as follows in Equations (1) and (2):

$$ACE_1 = \Delta P_{tie1-2} + B_1 \Delta f_1 \quad (1)$$

$$ACE_2 = \Delta P_{tie2-1} + B_2 \Delta f_2 \quad (2)$$

where,  $\Delta P_{tie1-2}$  and  $\Delta P_{tie2-1}$  represent the tie-line power exchange at area 1 and area 2,  $B_1$  and  $B_2$  are the bias frequency factors of area 1 and area 2 respectively,  $\Delta f_1$  is the deviation in frequency waveform in area 1, and also  $\Delta f_2$  is the deviation in frequency in area 2.

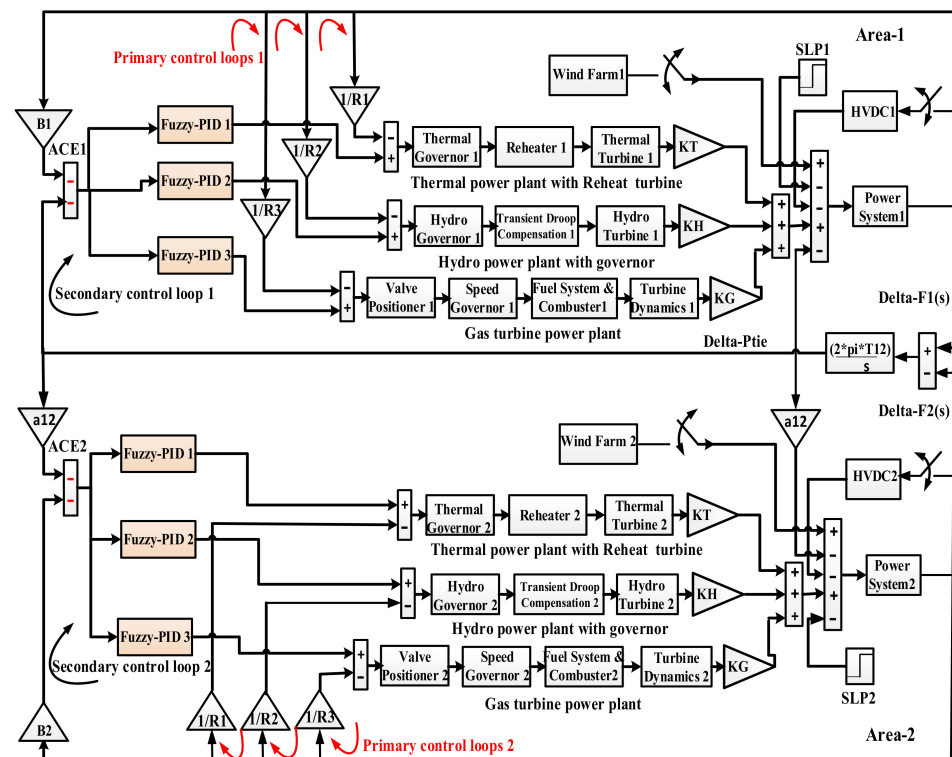
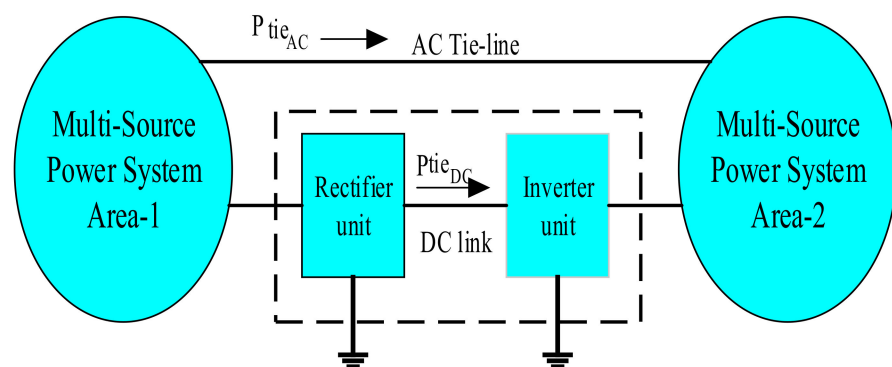


Figure 1. Transfer function model of the two-area interconnected power system. (see Appendix A).



**Figure 2.** Schematic diagram of the studied AC/DC interconnected power system.

**Table 2.** The parameters of two identical interconnected areas with standard values [49].

Symbol	Nominal Values
$B_i$	0.4312 MW/HZ
$T_{12}$	0.0433 MW
$R_1$	2.4 HZ/MW
$R_2$	2.4 HZ/MW
$R_3$	2.4 HZ/MW
$a_{12}$	-1
$K_T$	0.543478
$K_H$	0.326084
$K_G$	0.130438
$K_{ps}$	68.9566
$T_{ps}$	11.49 s
$T_{sg}$	0.08 s
$T_t$	0.3 s
$K_r$	0.3
$T_r$	10 s
$T_{gh}$	0.2 s
$T_{rs}$	5 s
$T_{rh}$	28.75 s
$T_w$	1 s
$b_g$	0.05
$c_g$	1
$Y_c$	1 s
$X_c$	0.6 s
$T_{cr}$	0.01 s
$T_{fc}$	0.23 s
$T_{cd}$	0.2 s
$K_{dc}$	1
$T_{dc}$	0.2 s

## 2.2. The Wind Farm Configuration

The model of the wind power has been built using the MATLAB/SIMULINK program. The random wind power is integrated with conventional units in both areas. According to the design of the wind power model, a white noise block is used to get a random speed which is multiplied by the wind speed as shown in Figure 3 [52]. The following equations illustrate the captured power from the wind by the rotor of the wind turbine [35].

$$P_{wt} = \frac{1}{2} \rho A_T v_w^3 C_p(\lambda, \beta) \quad (3)$$

$$C_p(\lambda, \beta) = C_1 \left( \frac{C_2}{\lambda_i} - C_3 \beta - C_4 \beta^2 - C_5 \right) \times e^{\frac{-C_6}{\lambda_i}} + C_7 \lambda_T \quad (4)$$

$$\lambda_T = \lambda_T^{OP} = \frac{\omega_T r_T}{V_W} \quad (5)$$

$$\frac{1}{\lambda_i} = \frac{1}{\lambda_T + 0.08\beta} - \frac{0.035}{\beta^3 + 1} \quad (6)$$

where,  $P_{wt}$  represents the captured output power of wind turbine,  $A_T$  is the swept area by the blades of turbine in  $m^2$ ,  $\rho$  is the air density (nominally  $1.22 \text{ Kg/m}^3$ ),  $V_W$  is the wind speed in m/s.

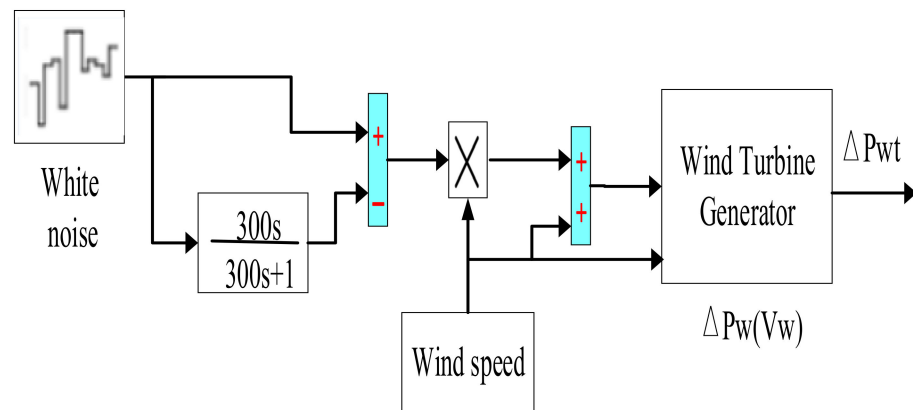


Figure 3. The wind power modeling using MATLAB/Simulink.

The climatic and geographical conditions where the studied wind turbine units located are the same. Thus, all previous parameters are applied to these units. The coefficient of rotor blades  $C_p$  based on turbine coefficients  $C_1$ – $C_7$  and it is a function on  $\lambda_T$  which refers to the optimum tip-speed ratio (TSR) and pitch angle  $\beta$ .  $\lambda_T$  is a function on the rotor speed ( $\omega_T$ ) and the blade length of rotor radius ( $r_T$ ). Moreover,  $\lambda_i$  is referring to the intermittent TSR. Table 3 shows the nominal parameter values of the wind turbine for the wind farm applied with the studied power system. Figure 4 shows the random output power of 130 wind turbine units of 750 KW which have been penetrated at both areas of the studied power system.

Table 3. The wind farm nominal parameters [52].

Parameters	Values
$P_{wt}$	750 KW
$V_W$	15 m/s
$A_T$	1648 $m^2$
$r_T$	22.9 m
$\omega_T$	22.5 rpm
$C_1$	−0.6175
$C_2$	116
$C_3$	0.4
$C_4$	0
$C_5$	5
$C_6$	21
$C_7$	0.1405

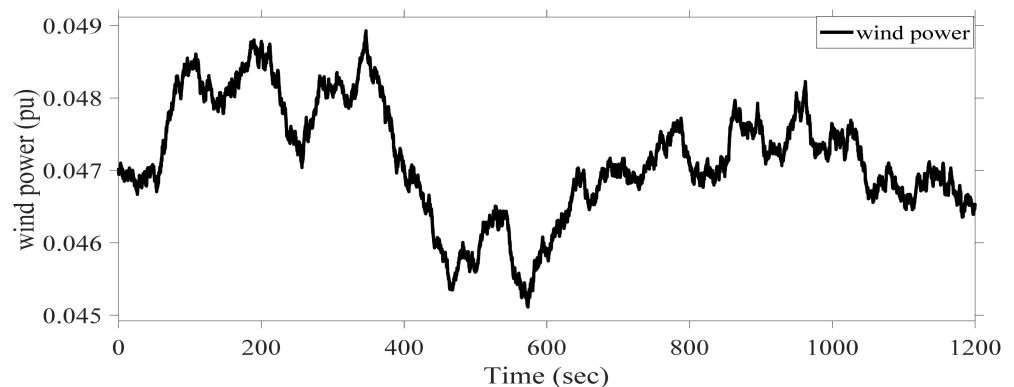


Figure 4. The wind power variation pattern.

### 3. Control Methodology and Problem Formulation

According to RESs penetration, system nonlinearities, and system uncertainties, it is essential to design good controller to improve the system performance during abnormal conditions. Hence, this study proposes fuzzy-PID controller to overcome any deviations resulted from previous considerations. Moreover, the proposed controller parameters have been selected based AOA algorithm.

#### 3.1. The Proposed Control Strategy

In this article, three fuzzy-PID controllers are proposed as responsible for extracting extra active power from thermal, hydro, and gas turbines respectively, when load disturbance occurs. In this regard, several studies have applied the trial and error runs method to detect the fuzzy-PID controller's input and output scaling factors [53]. Therefore, it is difficult to obtain the optimal parameter values which enhance the system performance through these trial and error methods. Therefore, this paper proposes designing the fuzzy-PID controller with the optimized input and output scaling factors. The AOA has been selected in this work to obtain the optimized values of the proposed controller's input and output scaling factors. Furthermore, Figure 5 shows the structure of the fuzzy-PID controller of the thermal, hydro, and gas units. It has two inputs; ACE and the change in ACE, and one output. The input scaling factors are  $K_1$  and  $K_2$  and the output scaling factors are  $K_3$  and  $K_4$  which are optimized via the proposed AOA.

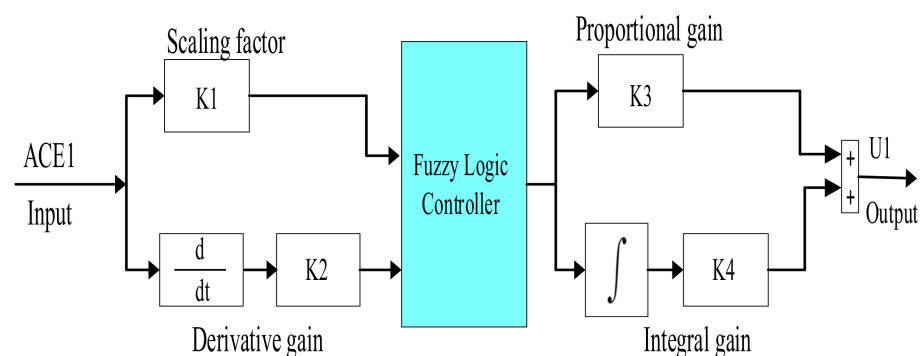
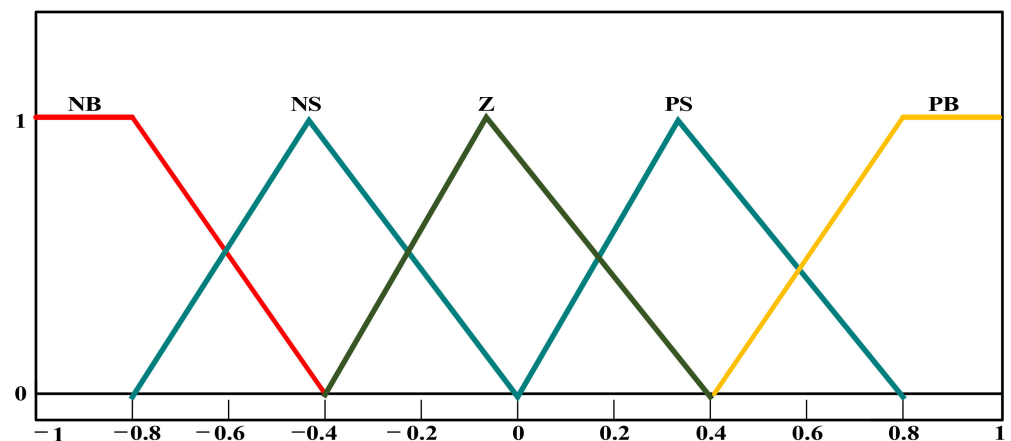


Figure 5. The proposed Fuzzy-PID controller diagram.

The fuzzy member ship may be triangular membership or Gaussian membership. Several studies applied the triangular membership due to its merits, where the triangular membership represents one of the attractive linear memberships of the fuzzy methodology, which is characterized by less computation time and simplicity [54]. The sensitivity increases when moving from linear membership functions to curvilinear membership functions (i.e., Gaussian-sigmoidal). Therefore, from the literature review of fuzzy logic,

the triangular membership is shown in more than 90% of practical applications of electrical systems which are used in input and output. In addition, this membership belongs to the first-order mathematical function, which is characterized by reducing the computational load. It is usually applied along with a PID controller and fully symmetric functions in input and output. The selection of fuzzy control parameters depends on the nature of the studied system and the knowledge of the designer of the system. So, the selection of fuzzy membership functions range is based on the prediction of the universe of discourse of input and output in the studied system [55]. Usually, the decision-maker is able to define the risk-free of input and output. Thus, the range intervals have been selected between  $[-1, 1]$  intervals, which is expected and doesn't need the input and output to go far away from this period to achieve more system stability. It is advisable to use the symmetric triangular MF with 50% overlap, and then apply a tuning procedure during which we can either change the left and/or right spread and/or overlap. This is to be continued till, getting satisfactory results [56]. In this work, five triangular membership functions of the fuzzy-PID controller are utilized namely negative big (NB), negative small (NS), zero (Z), positive small (PS), and positive big (PB). The triangular member function is shown in Figure 6, which is used for both inputs and output. Accordingly, the five memberships of the input and output variables of the fuzzy-PID controller, the generation of fuzzy output need 25 rules. These rules play an important role in the performance of the fuzzy-PID controller. These rules of the fuzzy logic controller are depicted in Table 4.



**Figure 6.** The Fuzzy Logic Controller membership functions of inputs and output.

**Table 4.** The Fuzzy rule base [50].

$ACE$	$\dot{ACE}$				
	NB	NS	Z	PS	PB
NB	NB	NB	NB	NS	Z
NS	NB	NB	NS	Z	PS
Z	NB	NS	Z	PS	PB
PS	NS	Z	PS	PB	PB
PB	Z	PS	PB	PB	PB

### 3.2. The Proposed Optimization Technique (AOA)

In 2020, a new meta-heuristic optimization technique namely the Arithmetic optimization algorithm (AOA) was invented by Laith et al. [57]. This technique is characterized by a high exploration search strategy, meaning that they can achieve the global optimum solution with few search agents. The distribution behavior of this technique is based on the main mathematical operations including; (Division ( $D$ ), Multiplication ( $M$ ), Addition ( $A$ ), and Subtraction ( $S$ )). According to meta-heuristic techniques, the former of this method

can make a wide coverage of searching space by using the number of search agents of the algorithm to avoid the local solution but for obtaining the global one. The AOA follows a detected methodology to obtain the global solution mentioned in the next steps:

Step 1: the proposed controller parameters in this paper have upper and lower boundaries; the population of the AOA method according to the main mathematical operations has been generated between these boundaries to achieve the global goal. The population of the AOA method can be formulated in Equation (7) as follows:

$$s(N, d) = rand(N, d) \times (UB - LB) + LB \quad (7)$$

where;  $N$  refers to the number of utilized search agents,  $d$  represents the variable dimensions (controller parameters),  $UB$  and  $L$  represent the upper and lower value of variables.

Step 2: The AOA method begins with candidate solutions ( $S$ ) generated randomly. The optimal obtained solution in each endeavor represents a solution near the global goal (target). The next matrix illustrates the position of solutions obtained.

$$s = \begin{bmatrix} s_{1,1} & s_{1,2} & \cdots & s_{1,d} \\ s_{2,1} & s_{2,2} & \cdots & s_{2,d} \\ \vdots & \vdots & \ddots & \vdots \\ s_{n,1} & s_{n,2} & \cdots & s_{N,d} \end{bmatrix} \quad (8)$$

Step 3: achieving the fitness solution among the obtained ones as mentioned in step 2. The fitness solution can be formulated in Equation (9) as follows:

$$f_{fitness} = [f_1 \ f_2 \ f_3 \ \dots \ f_N]^T \quad (9)$$

Step 4: before the AOA role begins, the search phase (exploration and exploitation) must be detected through the next formulation in Equation (10) of Math Optimizer Acceleration (MOA):

$$MOA(C\_Iter) = C\_Iter \times \left( \frac{Max - Min}{M\_Iter} \right) + Min \quad (10)$$

where;  $MOA(C\_Iter)$  refers to the value of function at the  $t$ th iteration,  $C\_Iter$  represents the current iteration. The current iteration is between among 1 and the maximum number of iterations ( $M\_Iter$ ) dimensions (controller parameters),  $Min$  and  $Max$  are the minimum and maximum values of the accelerated function.

Step 5: the mathematical calculation processes as (Division ( $D$ ) and Multiplication ( $M$ )) cannot reach the target easily according to their high dispersion. Accordingly, these strategies ( $D$  and  $M$ ) are utilized in the exploration search process. The first operator  $D$  in this phase is conditioned by  $r_2 < 0.5$  ( $r_2$  is a random number) and the second operator  $M$  will be neglected until the first one ends its task in searching for a solution near to the goal. Otherwise,  $M$  will lead the process instead of the first operator  $D$ . The exploration process is modeled in Equation (11):

$$X_{i,j}(C\_Iter + 1) \begin{cases} best(x_j) \div (MOP + \epsilon) \times ((UB_j - LB_j) \times \mu + LB_j), & r_2 < 0.5 \\ best(x_j) \times (MOP) \times ((UB_j - LB_j) \times \mu + LB_j), & otherwise \end{cases} \quad (11)$$

where,  $X_{i,j}(C\_Iter + 1)$  and  $X_{i,j}(C\_Iter)$  are the  $i$ th solution in the next iteration and the  $j$ th position of the  $i$ th solution at the current iteration,  $best(x_j)$  represents the  $j$ th position in the best-obtained solution,  $\epsilon$  is a small integer number,  $\mu$  is the control parameter to make adjusting in the process of search which is fixed equal to 0.5.

Step 6: deep search (exploitation) in this strategy using the mathematical operators (Subtraction ( $S$ ) and Addition ( $A$ )) has been applied to be near to the optimal solution and reach it after several iterations. The first operator  $S$  in this phase is conditioned by  $r_3 < 0.5$  ( $r_3$  is a random number) and the second operator  $A$  will be neglected until the first one

end its task in deep searching for obtaining the best solution. Otherwise,  $A$  will lead the process instead of the first operator  $S$ . The exploitation process is modeled in Equation (12):

$$X_{i,j}(C\_Iter + 1) \begin{cases} best(x_j) - (MOP) \times ((UB_j - LB_j) \times \mu + LB_j), & r3 < 0.5 \\ best(x_j) + (MOP) \times ((UB_j - LB_j) \times \mu + LB_j), & otherwise \end{cases} \quad (12)$$

Step 7: steps (3) to (6) are repeated until ending all iterations.

Step 8: The last step is to achieve the optimum solution which achieves the objective function.

Furthermore, Figure 7 illustrates the flow chart of the AOA which clarify the previous optimization steps.

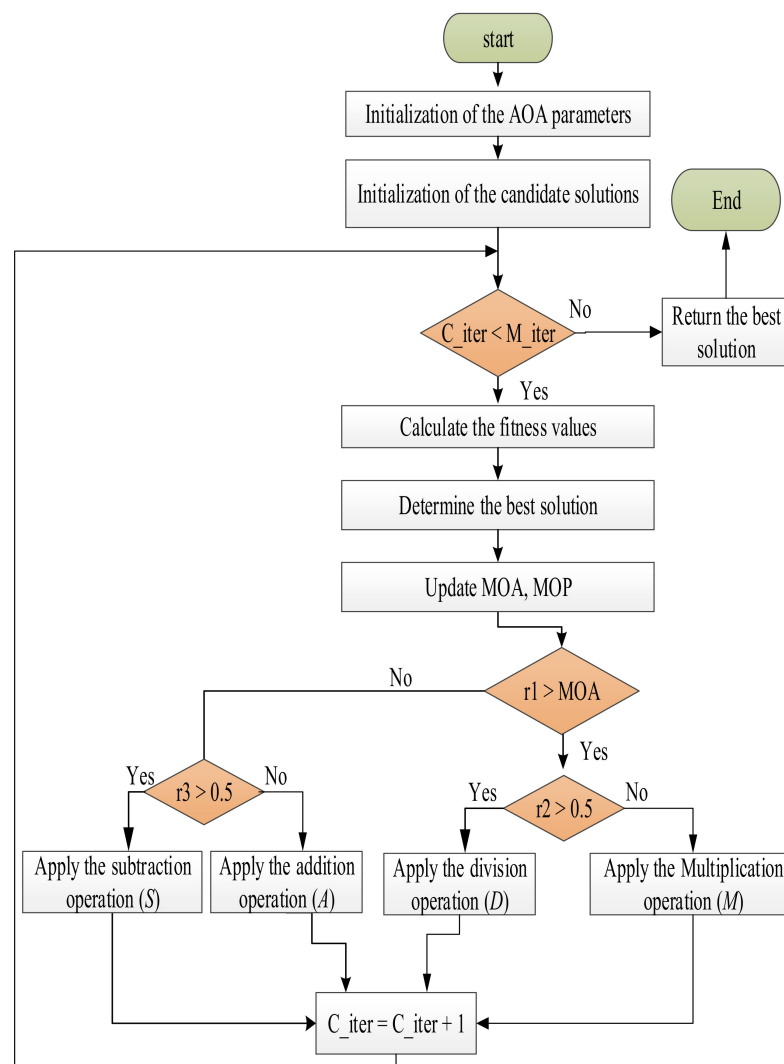


**Figure 7.** The flowchart of the AOA technique.

### 3.3. The Proposed Fuzzy-PID Control Strategy Based AOA Algorithm

The parameters of the proposed control strategy have been selected based on AOA algorithm to overcome any deviations related to the considered system. Moreover, the integral time absolute error (ITAE) function is utilized as an objective function ( $J$ ) of the proposed optimization algorithm. Furthermore, Equation (13) formulates the objective function  $J$  to minimize the deviations in system related to the frequency and tie-line power. The ITAE has been selected in this work according to its merits like, it has an additional time multiplies with the error function which makes the system faster than using other

objective functions forms (e.g., the integral square error (ISE) and the integral absolute error (IAE)). Also, the ITAE performance index has the advantage of settling the system, which is more quickly compared to other objective functions [49].

$$J = \text{ITAE} = \int_0^{T_{sim}} (|\Delta f1| + |\Delta f2| + |\Delta ptie|) \cdot t \times dt \quad (13)$$

where;  $T_{sim}$  is the simulation time. The flow chart of the proposed AOA is shown in Figure 8.

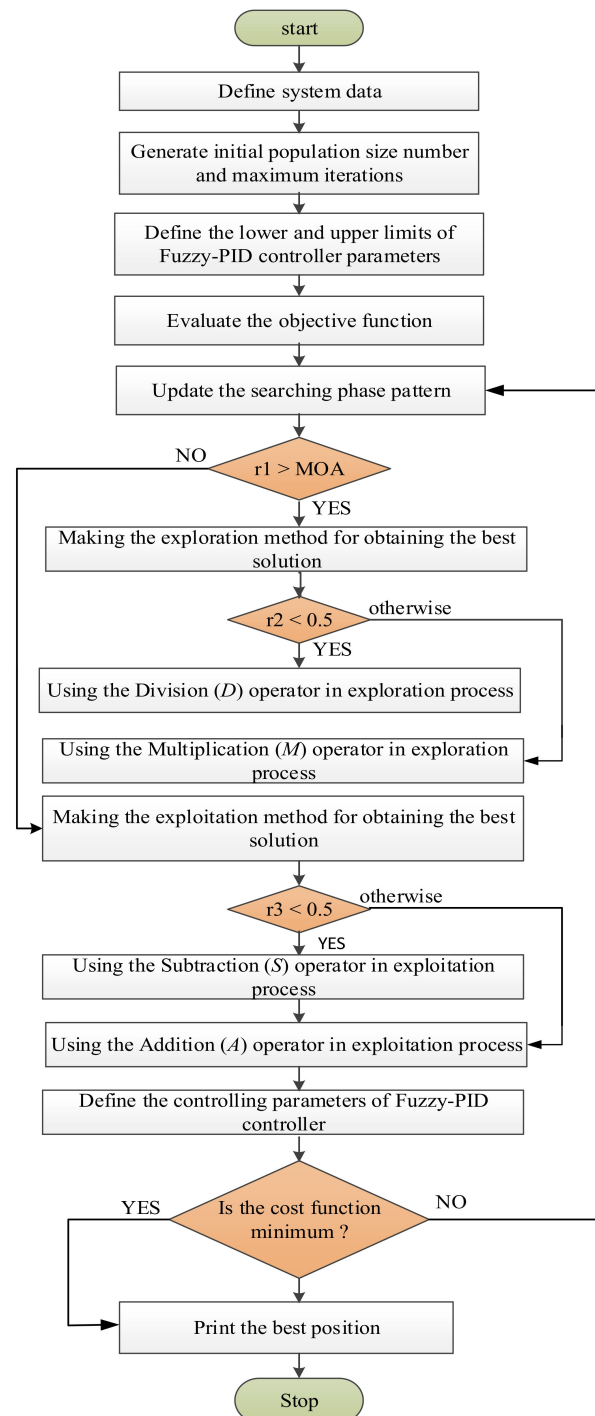
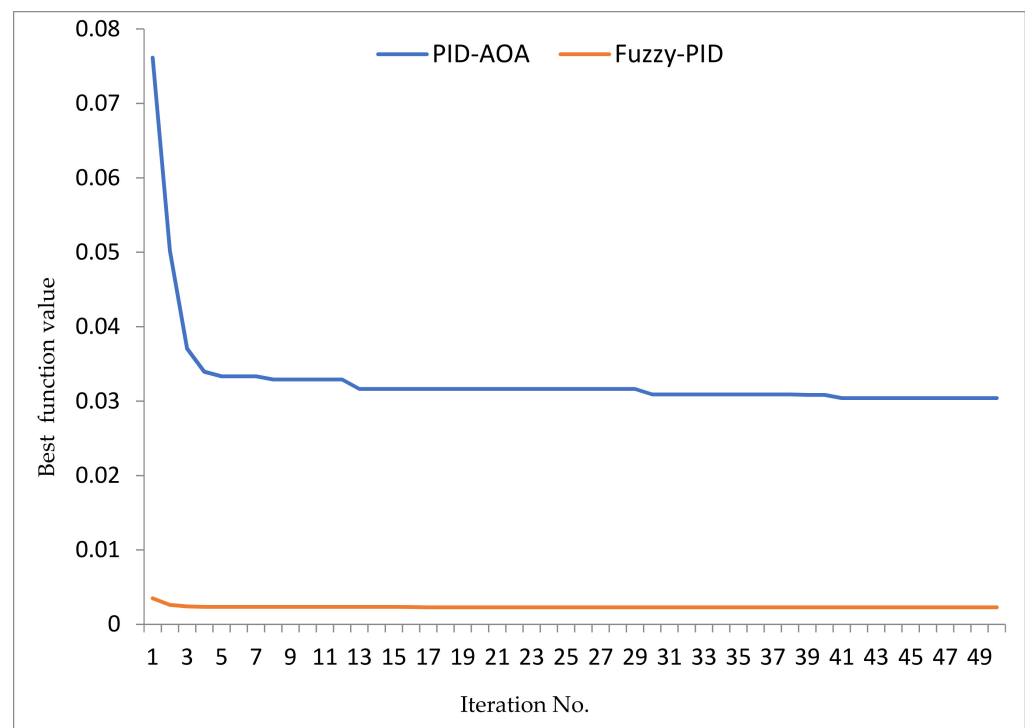


Figure 8. The flowchart of applying AOA technique with the proposed controller.

#### 4. Discussion and Simulation Results

The investigated system was built on a 2.60 GHz Intel (R) PC with 4.00 GB of RAM using the MATLAB/SIMULINK<sup>®</sup> software (R2019b) environment. In addition, the AOA has been written in the m file in order to tune the proposed controller parameters of the automatic load frequency control process. In this work, the performance of Fuzzy-PID and PID controllers that are applied to enhance the studied system performance using the AOA technique is measured according to the value of the best objective function over iterations. The initial values of the proposed AOA technique utilized in this work are; the number of search agents equals 30 and the number of maximum iterations equals 50. Also, the limitations of the proposed fuzzy-PID controller are in the range of [0, 10]. The convergence curve of the proposed fuzzy-PID controller compared to the PID controller using the AOA is shown in Figure 9. There is a clear difference between the performances of both controllers using the AOA technique. The behavior of the PID convergence curve can be summarized as follows: it begins with a high best function value (near to 0.08) and drops along iterations until it ends its career at the final iteration, reaching the best function value (near to 0.03). As for the Fuzzy-PID convergence curve behaviors, they start with a low best function value until it reaches a value (near to zero) to obtain an optimal objective function with more system stability. In general, the preference is for the Fuzzy-PID controller.



**Figure 9.** The convergence curve of the designed controllers based on the AOA.

All next simulation results ensure the effectiveness of the AOA in obtaining optimum controller parameters compared to other applied techniques as (PID controller based-DE [49], PID controller based-TLBO [50], and Fuzzy-PID controller based-LUS-TLBO [50]). For programming all mentioned optimization techniques, MATLAB/M-files matched with MATLAB /Simulink. All graphical and numerical numbers of obtained results are discussed in the next scenarios as follows:

##### 4.1. Studied Power System Performance Considering AC-Lines Connection Only

This scenario clarifies the dynamic system performance of the occurring deviation in frequency waveform at both areas and the tie-line power exchange between them with a 1%

step load perturbation (SLP) which applied to the first area only. The AC-line has tied both areas of the studied power system without any HVDC lines. Compared to other controllers applied previously by researchers, the proposed fuzzy-PID controller-based AOA proves its robustness in adjusting and stabilizing the power system frequency. Figures 10 and 11 show the frequency deviation performance at both areas of the studied system. The tie-line power exchange has been cleared in Figure 12. Table 5 indicates the optimal Fuzzy-PID controller parameters compared to other mentioned controllers with different optimization techniques. Additionally, the performance specifications; overshoot (OS), and undershoot (US) of the proposed Fuzzy-PID controller and followed controllers for the studied system are shown in Table 6. The percentage improvements in US and OS with different controllers are denoted in Table 7.

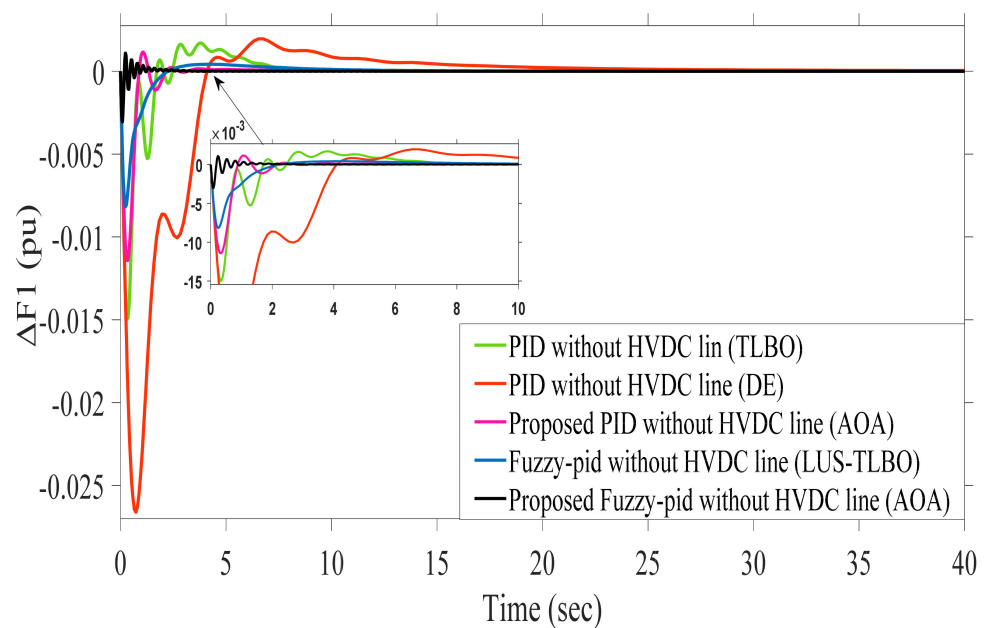


Figure 10. Dynamic response comparison results of  $\Delta f_1$  for scenario 4.1.

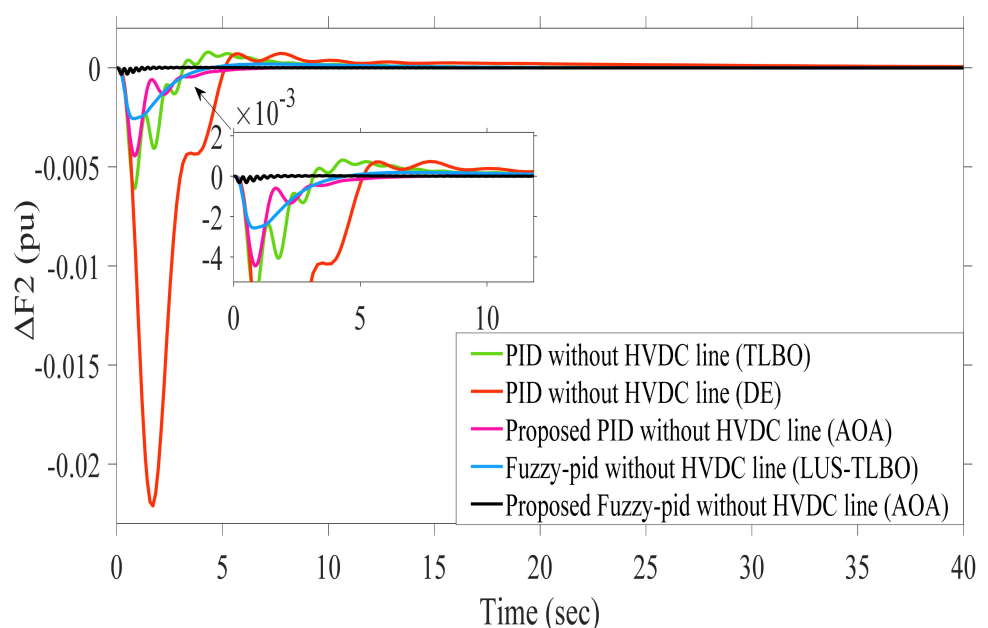


Figure 11. Dynamic response comparison results of  $\Delta f_2$  for scenario 4.1.

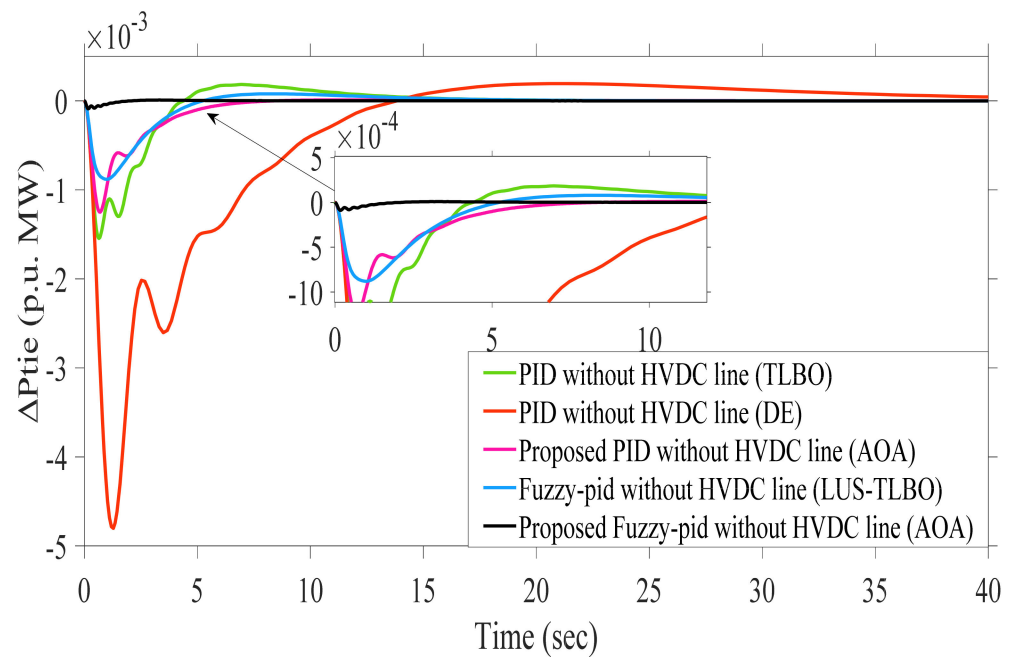


Figure 12. Dynamic response comparison results of  $\Delta p_{tie}$  for scenario 4.1.

Table 5. The optimal controllers' values for scenario 4.1.

ACE	Thermal				Hydro				Gas			
	k1	k2	k3	k4	k1	k2	k3	k4	k1	k2	k3	k4
Fuzzy-PID (LUS-TLBO) [50]	1.9985	1.9874	1.9679	1.9926	0.1002	1.1278	0.1032	0.7264	1.9782	1.0734	1.979	1.6516
Fuzzy-PID (AOA)	10	4.7015	4.7895	10	10	0.5402	0.01	10	9.4636	10	1.0988	10
PID (TLBO) [50]	4.1468	4.0771	2.0157	1.0431	0.6030	2.2866	4.7678	3.7644	4.9498			
PID (DE) [49]	0.779	0.2762	0.6894	0.5805	0.2291	0.7079	0.5023	0.9529	0.6569			
PID (AOA)	10	1.5975	2.7449	1.5975	0.0837	0.0875	10	10	1.2779			

Table 6. Performance evaluation of PID and Fuzzy-PID using all mentioned techniques for scenario 4.1.

Different Dynamic Responses	Fuzzy-PID Based LUS-TLBO OS & US $\times (10^{-3})$	Fuzzy-PID Based AOA OS & US $\times (10^{-3})$	PID Based-TLBO OS & US $\times (10^{-3})$	PID Based DE OS & US $\times (10^{-3})$	PID Based AOA OS & US $\times (10^{-3})$
Dynamic response of ( $\Delta F1$ )	0.5510 -8.9579	1.09 -3.059	1.7217 -19.7259	2.0347 -26.5777	1.158 -11.42
Dynamic response of ( $\Delta F2$ )	0.2119 -3.0119	0.03285 -0.321	0.4363 -12.7986	0.7722 -22.1421	0.02096 -4.443
Dynamic response of ( $\Delta P_{tie}$ )	0.0826 -0.9653	0.008388 -0.08917	0.1712 -3.0782	0.1935 -4.7595	0.01107 -1.249

Table 7. Percentage improvement in US and OS for all previous mentioned controllers with different techniques based on PID controller via DE for scenario 4.1.

Controller	$\Delta f_1$		$\Delta f_2$		$\Delta P_{tie}$	
	$U_{sh}$	$O_{sh}$	$U_{sh}$	$O_{sh}$	$U_{sh}$	$O_{sh}$
Fuzzy-PID (LUS-TLBO)	66.29	72.92	86.4	72.56	79.72	57.31
Fuzzy-PID (AOA)	88.49	46.43	98.55	95.75	98.13	95.67
PID (TLBO)	25.78	15.38	42.2	43.5	35.33	11.53
PID (AOA)	57.03	43.09	79.93	97.29	73.76	94.28

#### 4.2. Studied Power System Performance Considering AC-DC Lines Connection

The effect of adding an HVDC lines connection in addition to the existing AC lines to transmit the power alternately between both areas in the studied system is introduced in this scenario with a 1% step load perturbation (SLP) is applied to the first area only. The behavior of frequency at both areas and the tie-line power between the both is shown in Figures 13–15 respectively. Table 8 indicates different obtained controller parameters of the studied system in the presence of an HVDC line connection. It is observed that from Table 9, the proposed fuzzy-PID controller-based AOA achieves more system stability (less oscillation) by monitoring the system performance specifications such as OS and US than other mentioned controllers. Table 10 illustrates the percentage improvement in US and OS of area frequencies and tie-line power with different controllers.

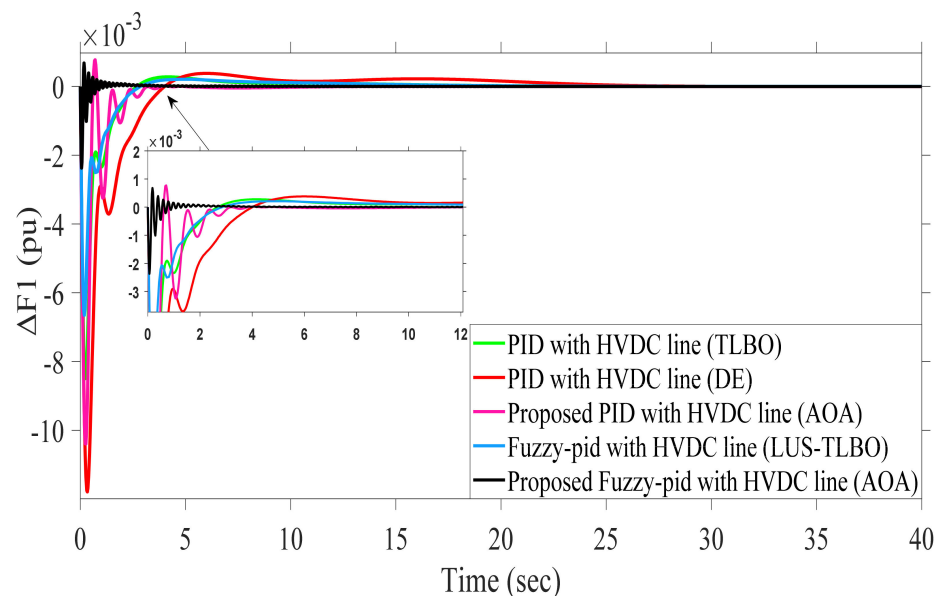


Figure 13. Dynamic response comparison results of  $\Delta f_1$  for scenario 4.2.

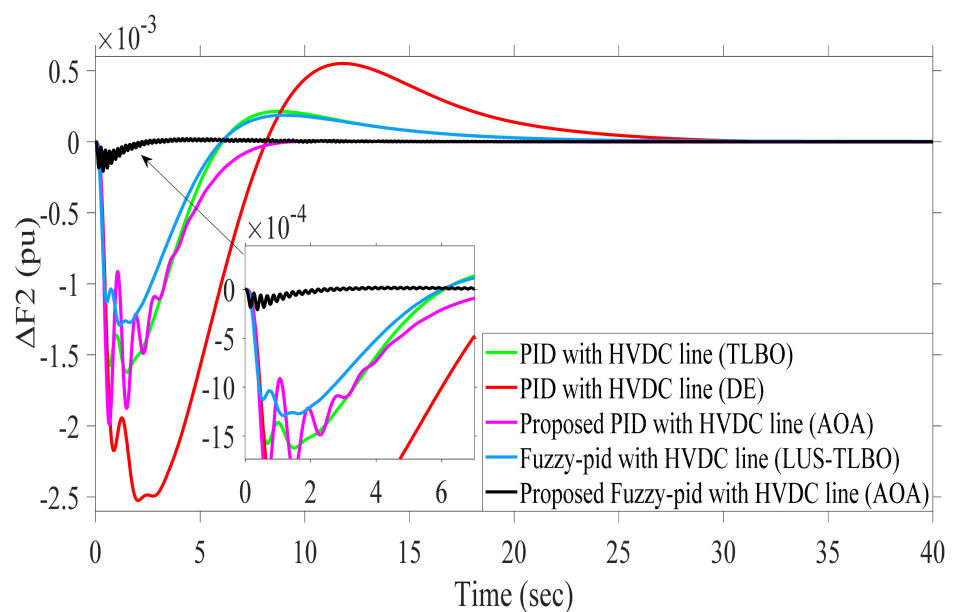


Figure 14. Dynamic response comparison results of  $\Delta f_2$  for scenario 4.2.

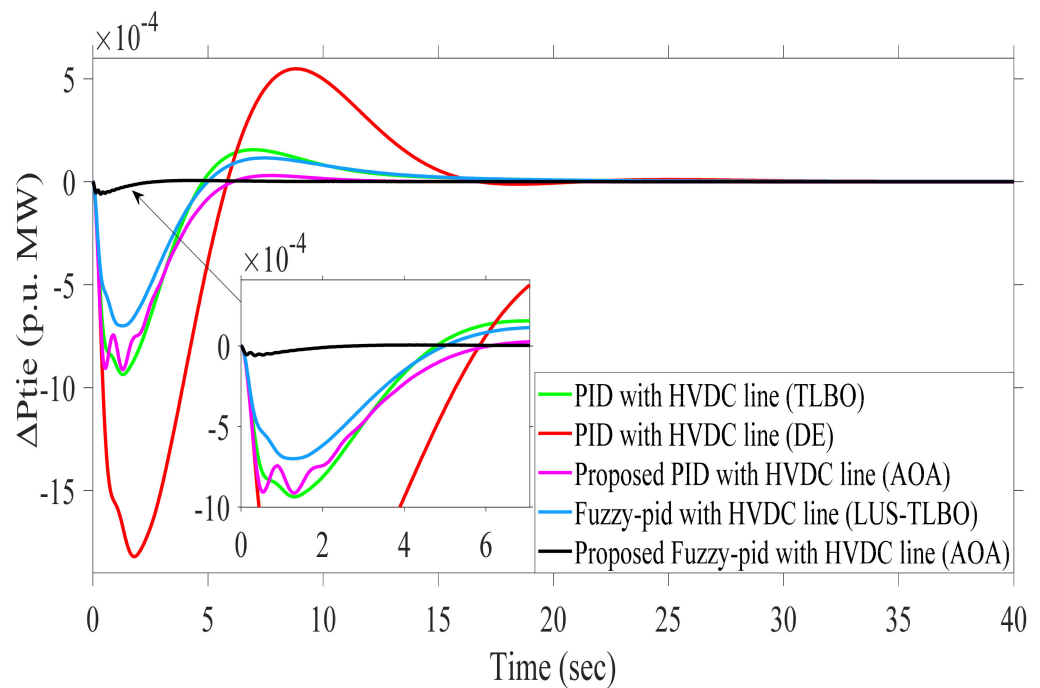


Figure 15. Dynamic response comparison results of  $\Delta P_{tie}$  for scenario 4.2.

Table 8. The optimal controllers' values for scenario 4.2.

ACE	Thermal				Hydro				Gas			
	k1	k2	k3	k4	k1	k2	k3	k4	k1	k2	k3	k4
Fuzzy-PID (LUS-TLBO) [50]	1.9995	1.9889	1.9975	1.9829	0.9668	1.2913	0.1001	1.9988	1.9969	1.1982	1.9867	1.9882
Fuzzy-PID (AOA)	10	9.9164 $k_p$	4.8295 $k_i$	10	10	0.01 $k_p$	4.9166 $k_i$	10	10	0.01 $k_p$	10	9.8531 $k_d$
PID (TLBO) [50]	5.0658	3.9658	2.417		0.7032	0.0220	0.0264		8.7211	7.4729	2.4181	
PID (DE) [49]	1.6929	1.9923	0.8269		1.77731	0.7091	0.4355		0.9094	1.9425	0.2513	
PID (AOA)	9.8739	1.2609	3.5014		10	0.0164	1.9788		1.2609	10	0.490	

Table 9. Performance evaluation of PID and Fuzzy-PID using all mentioned techniques for scenario 4.2.

Different Dynamic Responses	Fuzzy-PID Based LUS-TLBO OS & US $\times (10^{-3})$	Fuzzy-PID Based AOA OS & US $\times (10^{-3})$	PID Based-TLBO OS & US $\times (10^{-3})$	PID Based DE OS & US $\times (10^{-3})$	PID Based AOA OS & US $\times (10^{-3})$
Dynamic response of ( $\Delta F_1$ )	0.2809 −6.7244	0.6828 −2.373	0.2798 −8.497	0.3792 −11.6667	0.7707 −10.4
Dynamic response of ( $\Delta F_2$ )	0.2084 −1.4021	0.02112 −0.2083	0.2138 −1.624	0.5491 −2.5199	0.005693 −1.992
Dynamic response of ( $\Delta P_{tie}$ )	0.1353 −0.7292	0.006201 −0.05983	0.1557 −0.9366	0.5474 −1.8133	0.03018 −0.9134

Table 10. Percentage improvement in OS and US for all previous mentioned controllers with different techniques based on PID controller via DE for scenario 4.2.

Controller	$\Delta f_1$		$\Delta f_2$		$\Delta P_{tie}$	
	$U_{sh}$	$O_{sh}$	$U_{sh}$	$O_{sh}$	$U_{sh}$	$O_{sh}$
Fuzzy-PID (LUS-TLBO)	42.36	25.92	44.36	62.05	59.79	75.28
Fuzzy-PID (AOA)	79.66	80.06	91.73	96.15	96.7	98.87
PID (TLBO)	27.17	26.21	35.55	61.06	48.35	71.56
PID (AOA)	10.86	103.2	20.95	98.96	49.63	94.48

#### 4.3. Studied Power System Performance Considering AC-DC Lines Connection in Addition to Different Load Disturbances

The perturbation in load at the first area has been increased to be a 5% SLP instead of 1% to ensure the validation of the obtained fuzzy-PID controller parameters that mentioned in Table 4 in stabilizing the studied system frequency. The frequency deviation of both areas and the exchanged power between them is shown in Figures 16–18 respectively. The OSs and USs values of oscillations at frequency waveform at area 1 and area 2 are mentioned in Table 11; in addition to values of tie-line power. Table 12 shows the percentage improvement in OS and US with different controllers in the case of increasing SLP to 0.05 p.u. It can be said that the studied system became more stable using the proposed fuzzy-PID controller-based AOA compared to the fuzzy-PID controller-based LUS-TLBO and PID controller based on TLBO, DE, and AOA.

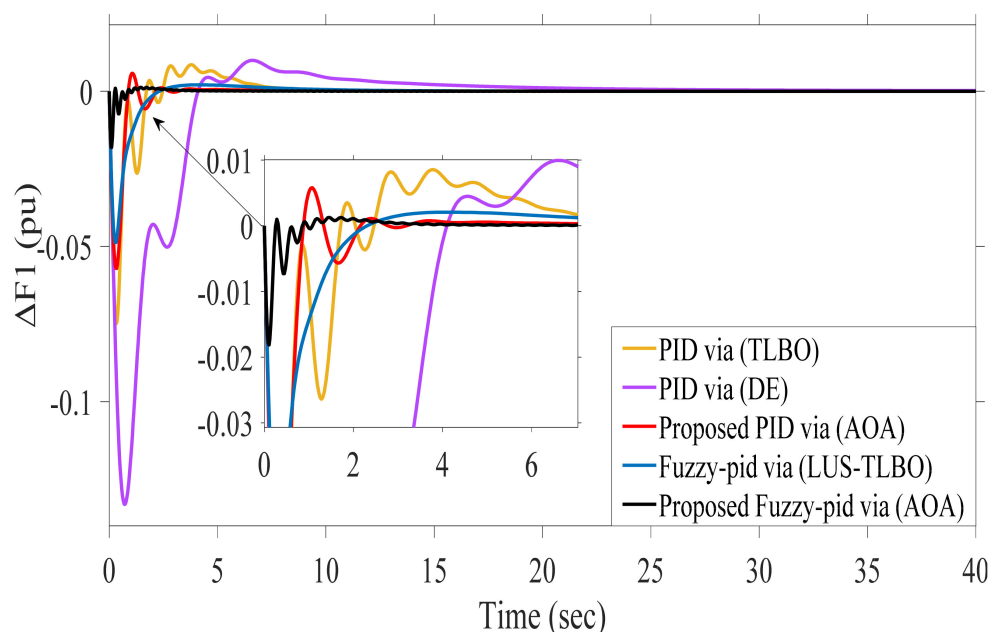


Figure 16. Dynamic response comparison results of  $\Delta f_1$  for scenario 4.3.

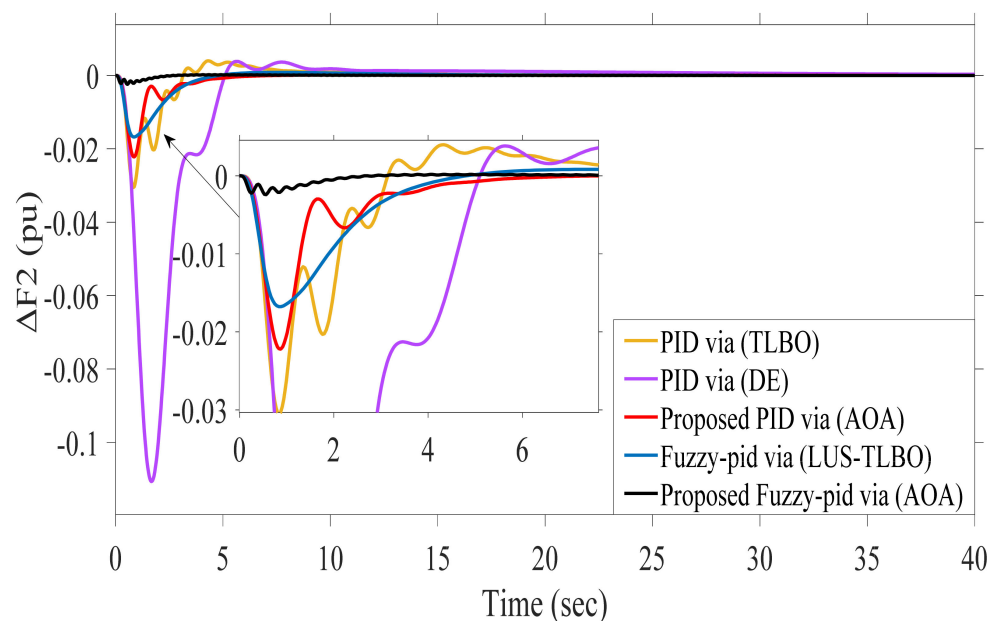


Figure 17. Dynamic response comparison results of  $\Delta f_2$  for scenario 4.3.

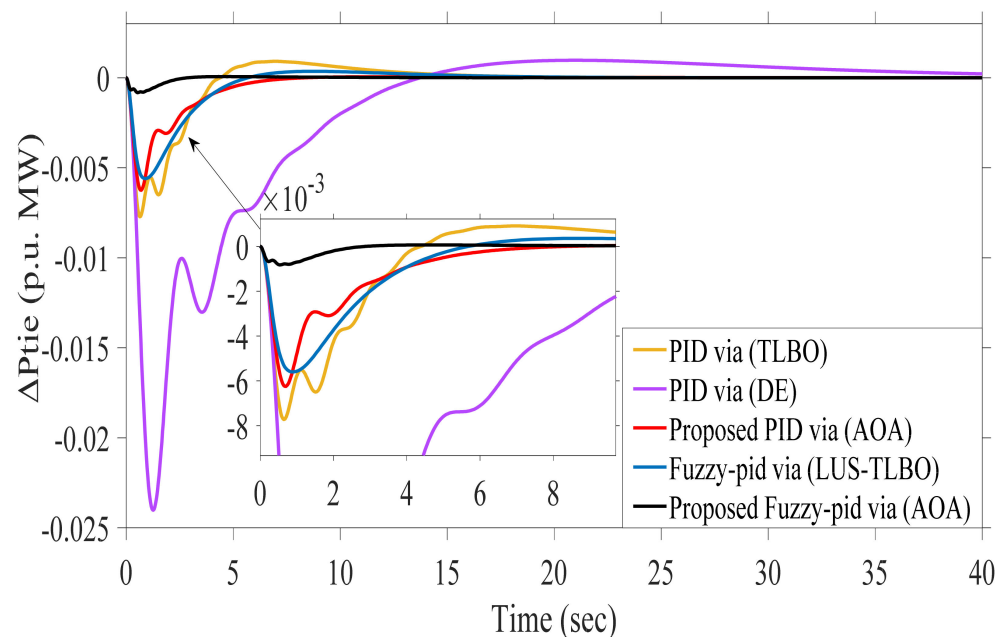


Figure 18. Dynamic response comparison results of  $\Delta p_{tie}$  for scenario 4.3.

Table 11. Performance evaluation of PID and Fuzzy-PID using all mentioned techniques for scenario 4.3.

Different Dynamic Responses	Fuzzy-PID Based LUS-TLBO OS & US $\times (10^{-3})$	Fuzzy-PID Based AOA OS & US $\times (10^{-3})$	PID Based-TLBO OS & US $\times (10^{-3})$	PID Based DE OS & US $\times (10^{-3})$	PID Based AOA OS & US $\times (10^{-3})$
Dynamic response of ( $\Delta F_1$ )	2.063 −48.74	1.28 −18.13	8.552 −74.85	9.956 −133.1	5.795 −57.07
Dynamic response of ( $\Delta F_2$ )	0.8297 −16.77	0.1825 −2.418	3.981 −30.52	3.823 −110.7	0.1048 −22.21
Dynamic response of ( $\Delta P_{tie}$ )	0.359 −5.6	0.06577 −0.8255	0.9155 −7.719	0.9719 −24.02	0.05535 −6.245

Table 12. Percentage improvement in US and OS for all previous mentioned controllers with different techniques based on PID controller via DE for scenario 4.3.

Controller	$\Delta f_1$		$\Delta f_2$		$\Delta P_{tie}$	
	$U_{sh}$	$O_{sh}$	$U_{sh}$	$O_{sh}$	$U_{sh}$	$O_{sh}$
Fuzzy-PID (LUS-TLBO)	63.38	79.28	84.85	78.30	76.79	63.06
Fuzzy-PID (AOA)	86.38	87.14	97.82	95.23	96.56	93.23
PID (TLBO)	43.76	14.10	72.43	−4.13	35.33	5.8
PID (AOA)	57.12	41.79	79.94	97.26	74.00	94.30

#### 4.4. Studied Power System Performance Considering the Effect of System Parameters' Variations

The robustness of the studied power system has been tested by making a variation of system parameters such as thermal governor time constant at both areas, thermal turbine time constant at both areas and hydro governor time constant simultaneously in the range of +25% and −25% from their nominal values reported in Table 2. These variations ensure that, the obtained fuzzy-PID controller parameters based AOA that mentioned in Table 4 can efficiently damp and overcome the oscillations and achieve more system stability under system parameters variation. The dynamic performance of both areas frequencies and tie-line power exchange after  $\pm 25\%$  system parameters variation is illustrated in Figures 19–21 respectively.

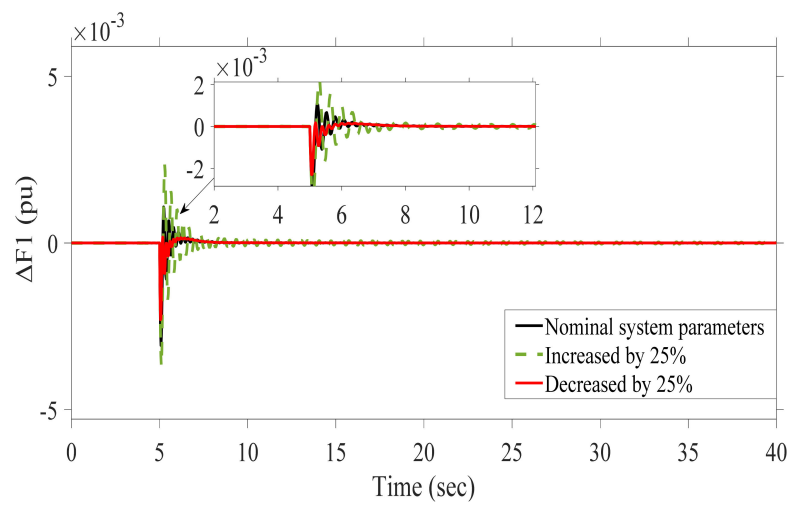


Figure 19. Dynamic response comparison results of  $\Delta f_1$  for scenario 4.4.

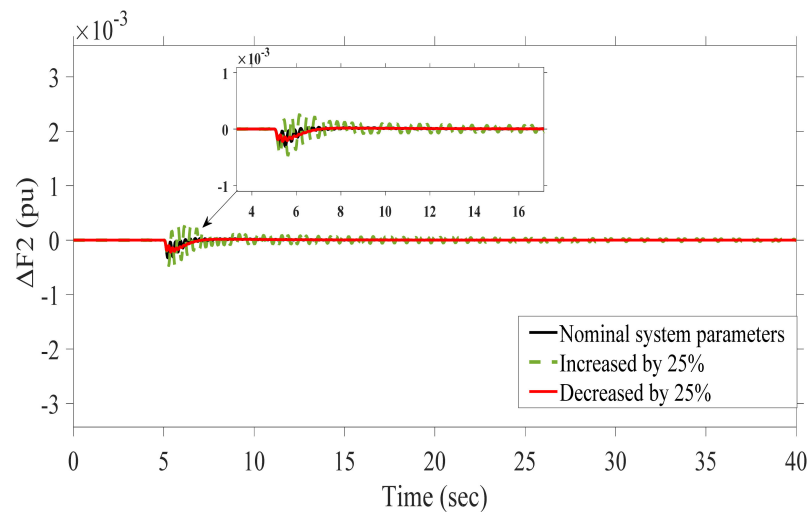


Figure 20. Dynamic response comparison results of  $\Delta f_2$  for scenario 4.4.

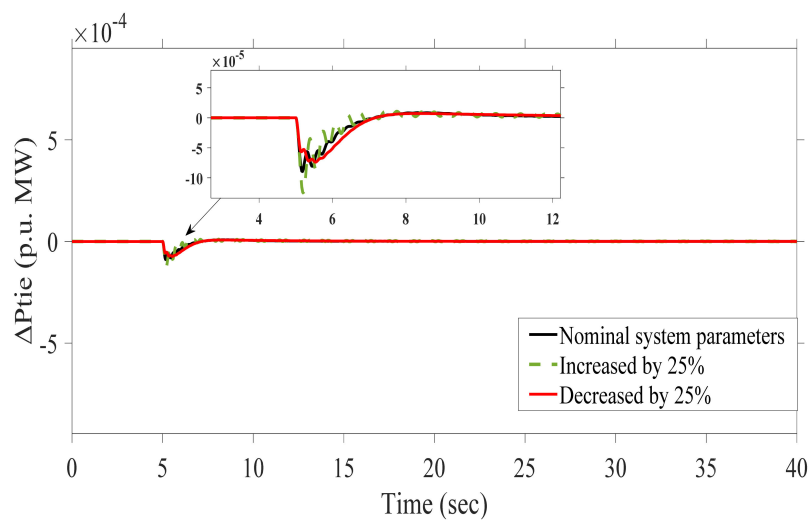


Figure 21. Dynamic response comparison results of  $\Delta p_{tie}$  for scenario 4.4.

#### 4.5. Studied Power System Performance Considering Wind Power Penetration

##### 4.5.1. Case A

The penetration of wind power at both areas of the studied system is tested in this scenario at nominal system parameters. Both wind farms have the same power rating and penetrated the studied system at the same time ( $t = 0$  s) with the instant of 1% load variation. This scenario is applied to ensure the robustness of the proposed fuzzy-PID controller based AOA that mentioned in Table 4 in achieving system stability in existing wind energy. All dynamic system performance (both-area frequencies and tie power) have been plotted in Figures 22–24 respectively. Table 13 illustrates the OSs and USs behavior of both areas frequencies and tie-line power with penetrating of wind energy at the studied power system. Also, Table 14 indicates the percentage performance in US and OS with different controllers.

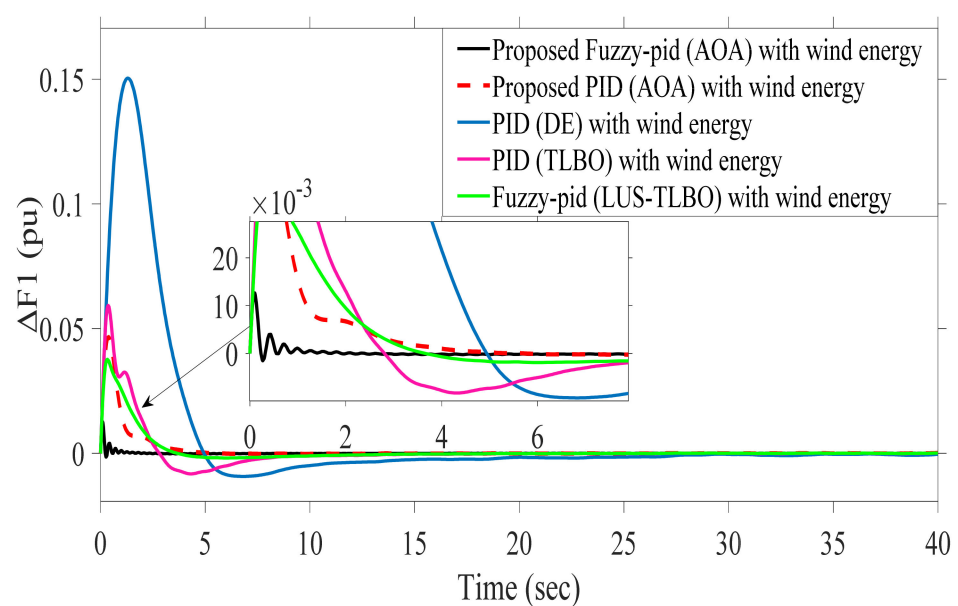


Figure 22. Dynamic response comparison results of  $\Delta f_1$  for scenario 4.5.1: case A.

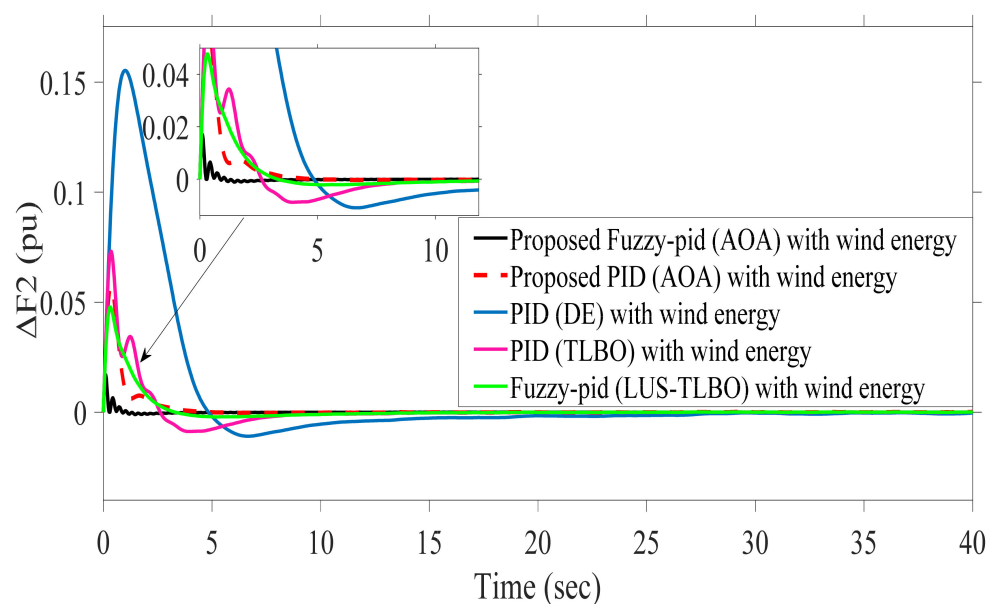


Figure 23. Dynamic response comparison results of  $\Delta f_2$  for scenario 4.5.1: case A.

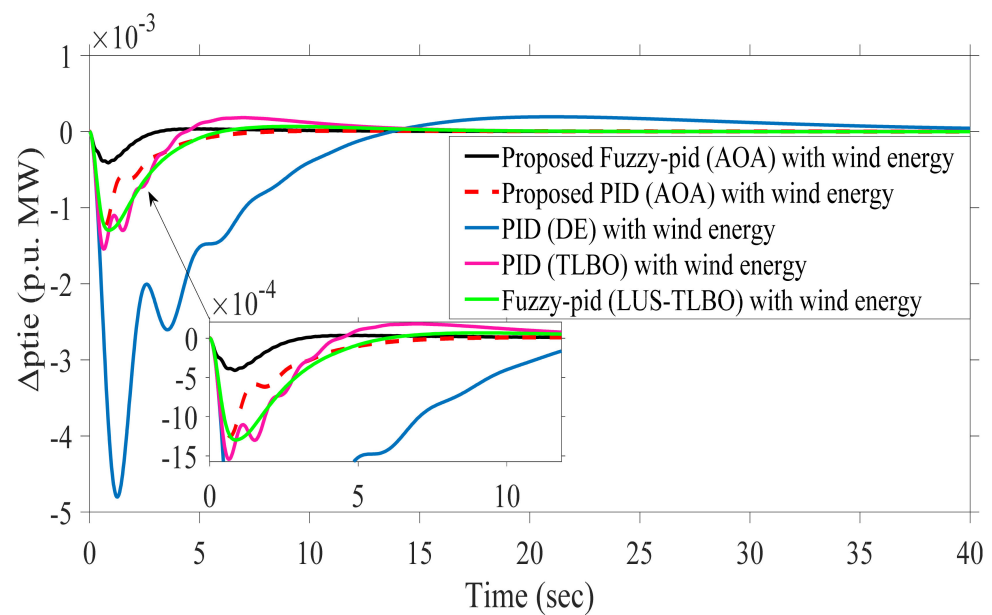


Figure 24. Dynamic response comparison results of  $\Delta p_{tie}$  for scenario 4.5.1: case A.

Table 13. Performance evaluation of PID and Fuzzy-PID using all mentioned techniques for scenario 4.5.1: case A.

Different Dynamic Responses	Fuzzy-PID Based LUS-TLBO OS & US $\times (10^{-3})$	Fuzzy-PID Based AOA OS & US $\times (10^{-3})$	PID Based-TLBO OS & US $\times (10^{-3})$	PID Based DE OS & US $\times (10^{-3})$	PID Based AOA OS & US $\times (10^{-3})$
Dynamic response of ( $\Delta F_1$ )	37.7 −1.88	12.69 −1.526	59.25 −8.257	150.5 −9.28	46.6 −0.2713
Dynamic response of ( $\Delta F_2$ )	47.75 −2.163	17.1 −1.106	73.12 −8.793	155.4 −10.92	56.86 −0.3124
Dynamic response of ( $\Delta P_{tie}$ )	0.06752 −1.297	0.0361 −0.41	0.1831 −1.543	0.1944 −4.804	0.01107 −1.249

Table 14. Percentage improvement in US and OS for all previous mentioned controllers with different techniques based on PID controller via DE for scenario 4.5.1: case A.

Controller	$\Delta f_1$		$\Delta f_2$		$\Delta P_{tie}$	
	$U_{sh}$	$O_{sh}$	$U_{sh}$	$O_{sh}$	$U_{sh}$	$O_{sh}$
Fuzzy-PID (LUS-TLBO)	79.74	74.95	80.19	69.27	73.00	65.27
Fuzzy-PID (AOA)	83.56	91.57	89.87	89.00	91.47	81.43
PID (TLBO)	11.02	60.63	19.48	52.95	67.88	5.81
PID (AOA)	97.08	69.04	97.14	63.41	74.00	94.31

#### 4.5.2. Case B

In this case, the studied power system is stabilized until load variation occurred at ( $t = 40$  s) in the first area. Also, the wind farm at the first area shared generated power at ( $t = 300$  s) then the wind energy from the wind farm at the second area enter to feed the system at ( $t = 600$  s). It is observed that the obtained fuzzy-PID controller parameters based AOA that mentioned in Table 5 achieve more system stability than those obtained by LUS-TLBO. Also, the fuzzy-PID controller parameters based on the AOA recover the studied system and back it to nominal operation process faster than PID controller based TLBO, DE, and AOA. Figures 25–27 show the dynamic performance of area frequencies and the exchanged tie-line power when sharing wind energy to the studied system at different instants ( $t = 300$  s,  $t = 600$  s). Table 15 extract the effectiveness of the fuzzy-PID-based AOA compared to other mentioned controllers by showing the OSs and USs of both

areas frequencies and the tie-line power. The percentage improvement in US and OS with different controllers via various techniques is mentioned in Table 16.

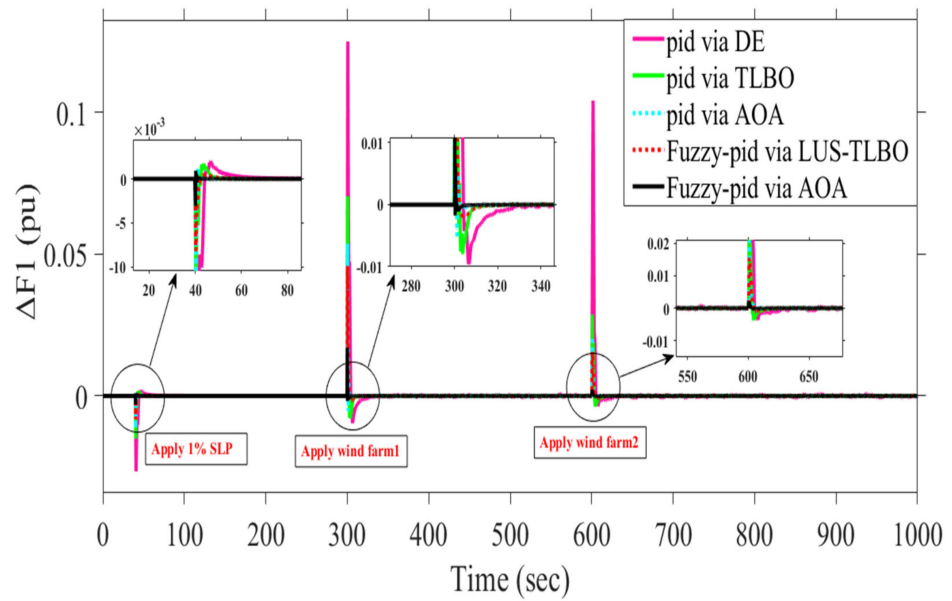


Figure 25. Dynamic response comparison results of  $\Delta f_1$  for scenario 4.5.2: case B.

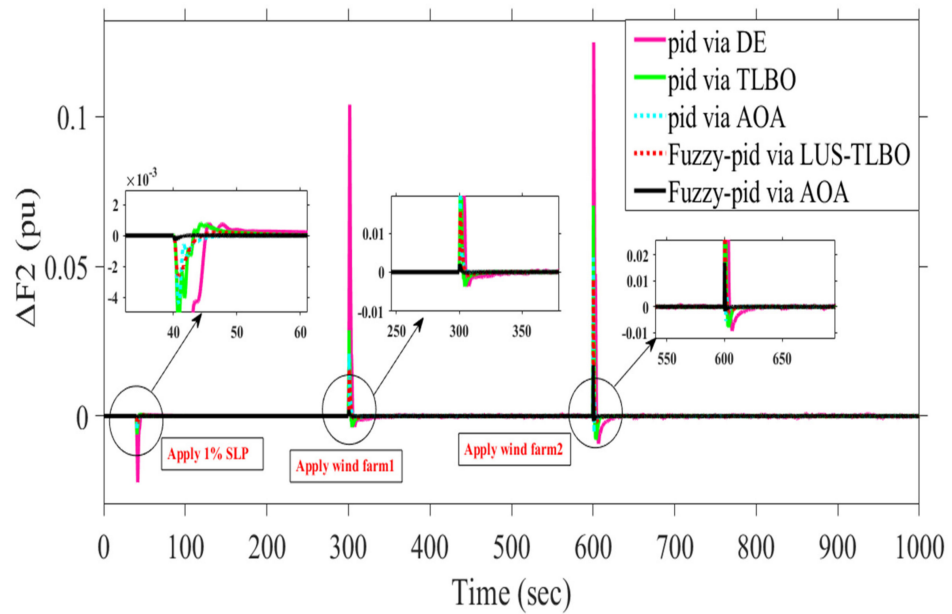


Figure 26. Dynamic response comparison results of  $\Delta f_2$  for scenario 4.5.2: case B.

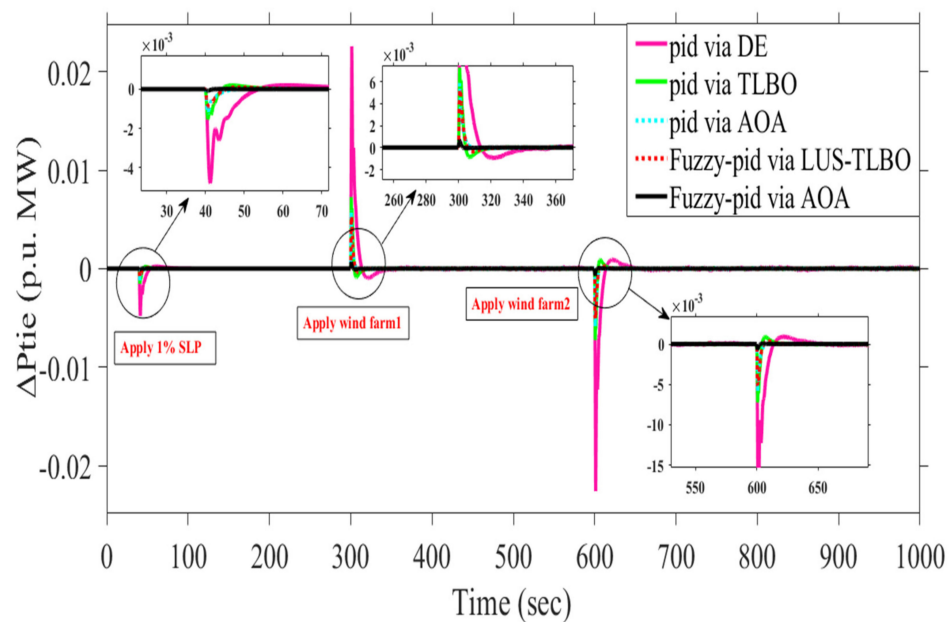


Figure 27. Dynamic response comparison results of  $\Delta p_{tie}$  for scenario 4.5.2: case B.

Table 15. Performance evaluation of PID and Fuzzy-PID using all mentioned techniques for scenario 4.5.2: case B.

Different Dynamic Responses	Fuzzy-PID Based LUS-TLBO OS & US $\times (10^{-3})$	Fuzzy-PID Based AOA OS & US $\times (10^{-3})$	PID Based-TLBO OS & US $\times (10^{-3})$	PID Based DE OS & US $\times (10^{-3})$	PID Based AOA OS & US $\times (10^{-3})$
Dynamic response of ( $\Delta F1$ )	45.73 −8.18	16.98 −3.058	70.37 −14.98	124.9 −26.6	53.66 −11.43
Dynamic response of ( $\Delta F2$ )	45.57 −2.586	17.01 −1.738	70.31 −7.94	124.8 −22.13	53.68 −5.42
Dynamic response of ( $\Delta P_{tie}$ )	5.233 −5.199	0.7004 −0.7178	7.246 −7.257	22.57 −22.60	5.867 −5.874

Table 16. Percentage improvement in US and OS for all previous mentioned controllers with different techniques based on PID controller via DE for scenario 4.5.2: case B.

Controller	$\Delta f_1$		$\Delta f_2$		$\Delta P_{tie}$	
	$U_{sh}$	$O_{sh}$	$U_{sh}$	$O_{sh}$	$U_{sh}$	$O_{sh}$
Fuzzy-PID (LUS-TLBO)	69.25	63.39	88.31	63.49	77.00	76.81
Fuzzy-PID (AOA)	88.50	86.41	92.15	86.37	96.82	96.90
PID (TLBO)	43.68	43.66	64.12	43.66	67.89	67.89
PID (AOA)	57.03	57.04	75.51	56.99	74.01	74.00

### 5. Conclusions

In this paper, there are main points that have been included, which can be summarized as follows:

- The proposed fuzzy-PID controller has been implemented on the two-area interconnected multi-source power systems that include thermal, hydro, and gas power plants for tackling the LFC problem.
- The selection the of the proposed controller parameters has been made via a new meta-heuristic optimization technique, which is known as an arithmetic optimization algorithm, to get the optimal solution which leads to stabilizing the system performance. Applying HVDC link in addition to AC links to overcome the demerits of the AC tie-lines.

- Considering several challenges during designing the proposed control parameters such as (i.e., system uncertainties, different load variations, and different levels of wind power penetration).
- Applying different scenarios to validate the robustness of the proposed fuzzy-PID controller than other previous controllers.
- The proposed AOA has tuned the fuzzy-PID controller to achieve a better disturbance rejection ratio than a newly published technique namely a hybrid Local Unimodal Sampling and Teaching Learning Based Optimization using also Fuzzy-PID controller. On the other hand, PID controller-based-AOA gets more system stability than which utilized in previous research work optimized by Differential Evolution, TLBO.
- The system performance has been enhanced by 90.76% by applying the proposed fuzzy-PID controller based on the AOA algorithm in comparison with the fuzzy-PID controller based on the LUS-TLBO algorithm.
- The presence of an HVDC link in parallel with an AC link improved system performance by 95.42% when compared to using only an AC tie-line.
- According to the analysis and simulation results, the Fuzzy-PID controller based on the AOA algorithm gives better results in terms of system stability and security in comparison with other previous control techniques.

There are some points will be taken in consideration in the future work and can be summarized as follows:

- Increasing the penetration level of renewable energy sources in the considered system.
- Applying different types of energy storage devices to study its effect on LFC problem.
- Improving of different recent optimization techniques to achieve the desired control parameters that lead to satisfied performance.

**Author Contributions:** Conceptualization, A.H.A.E., M.K., G.M. and S.K.; data curation, I.B.M.T.; formal analysis, A.H.A.E., M.K. and G.M.; funding acquisition, I.B.M.T. and S.K.; investigation, A.H.A.E., M.K. and G.M.; methodology, I.B.M.T. and S.K.; project administration, A.H.A.E., M.K. and G.M.; resources, I.B.M.T. and S.K.; supervision, S.K. and I.B.M.T.; validation, A.H.A.E., M.K. and G.M.; visualization, A.H.A.E., M.K. and G.M.; writing—original draft, A.H.A.E., M.K. and G.M.; writing—review and editing, I.B.M.T. and S.K. All authors have read and agreed to the published version of the manuscript.

**Funding:** Taif University Researchers Supporting Project Number (TURSP-2020/61), Taif University, Taif, Saudi Arabia.

**Institutional Review Board Statement:** Not applicable.

**Informed Consent Statement:** Not applicable.

**Data Availability Statement:** Not applicable.

**Acknowledgments:** The authors would like to acknowledge the financial support received from Taif University Researchers Supporting Project Number (TURSP-2020/61), Taif University, Taif, Saudi Arabia.

**Conflicts of Interest:** The authors declare that there is no conflict of interest.

## Nomenclature

Symbols	Parameters
FLC	Fuzzy logic control
PID	Proportional-Integral-Derivative
AOA	Arithmetic Optimization Algorithm
LFC	Load Frequency Control
HVDC	High Voltage Direct Current
RESs	Renewable Energy Sources

CEs	Conventional Energy Sources
DE	Differential Evolution
LUS	Local Unimodal Sampling
TLBO	Teaching Learning-based Optimization
OS	overshoot
US	undershoot
SLP	Step load perturbation
$\Delta P_{wt}$	Wind turbine output power
$\rho$	The air density
$A_T$	The swept area by the blades of turbine
$V_W$	The wind speed
$C_p$	The coefficient of rotor blades
$C_1$ – $C_7$	The turbine coefficients
$\beta$	The pitch angle
$r_T$	The radius of rotor
$\omega_T$	The rotor speed
$\lambda_T$	The optimum tip-speed ratio
$\lambda_i$	The intermittent tip-speed ratio
$B_1$	Frequency bias factor of Area 1
$B_2$	Frequency bias factor of Area 2
$\Delta f_1$	Deviation in frequency waveform in area 1
$\Delta f_2$	Deviation in frequency waveform in area 2
$\Delta P_{tie1-2}$	Tie-line power exchange at area 1
$\Delta P_{tie2-1}$	Tie-line power exchange at area 2
$T_{12}$	Coefficient of synchronizing
$R_1$	Regulation constant of thermal power plant
$R_2$	Regulation constant of hydro power plant
$R_3$	Regulation constant of gas turbine
$a_{12}$	Control Area Capacity Ratio
$K_T$	Participation factor for thermal unit
$K_H$	Participation factor for hydro unit
$K_G$	Participation factor for gas unit
$K_{ps}$	Gain constant of power system
$T_{ps}$	Time constant of power system
$T_{sg}$	Governor time constant
$T_t$	Turbine Time Constant
$K_r$	Gain of reheater steam turbine
$T_r$	Time Constant of reheater steam turbine
$T_{gh}$	Speed governor time constant of hydro turbine
$T_{rs}$	Speed governor reset time of hydro turbine
$T_{rh}$	Transient droop time constant of hydro turbine speed governor
$T_w$	Nominal string time of water in penstock
$b_g$	Gas turbine constant of valve positioner
$c_g$	Valve positioner of gas turbine
$Y_c$	Lag time constant of gas turbine speed governor
$X_c$	Lead time constant of gas turbine speed governor
$T_{cr}$	Gas turbine combustion reaction time delay
$T_{fc}$	Gas turbine fuel time constant
$T_{cd}$	Gas turbine compressor discharge volume-time constant
$K_{dc}$	Gain of HVDC link
$T_{dc}$	Time constant of hvdc link
ITAE	Integral time absolute error
ISE	Integral square error
IAE	Integral absolute error
$K_1$	Input scaling factor
$K_2$	Derivative input gain
$K_3$	Proportional output gain
$K_4$	Integral output gain

NB	Negative big
NS	Negative small
Z	Zero
PB	Positive big
PS	Positive small
UB	Upper boundary value
LB	Lower boundary value

## Appendix A

**Table A1.** Transfer functions included in the studied system.

Control Block	Transfer Functions
Thermal Governor	$\frac{1}{T_{sg}.s+1}$
Reheater of Thermal Turbine	$\frac{K_{r*}Tr.s+1}{Tr.s+1}$
Thermal Turbine	$\frac{1}{Tt.s+1}$
Hydro Governor	$\frac{1}{Tgh.s+1}$
Transient Droop Compensation	$\frac{T_{rs}.s+1}{T_{rh}.s+1}$
Hydro Turbine	$\frac{-Tws+1}{0.5*Tw.s+1}$
Valve Positioner of Gas Turbine	$\frac{1}{bg.s+cg}$
Speed Governor of Gas Turbine	$\frac{Xc.s+1}{Yc.s+1}$
Fuel System and Combustor	$\frac{Tcr.s+1}{Tfc.s+1}$
Gas Turbine Dynamics	$\frac{1}{Tcd.s+1}$
Power System 1	$\frac{Kps1}{Tps1.s+1}$
Power System 2	$\frac{Kps2}{Tps2.s+1}$
HVDC 1	$\frac{Kdc1}{Tdc1.s+1}$
HVDC 2	$\frac{Kdc2}{Tdc2.s+1}$

## References

- Mosaad, M.I.; El-Raouf, M.O.A.; Al-Ahmar, M.A.; Bendary, F.M. Optimal PI controller of DVR to enhance the performance of hybrid power system feeding a remote area in Egypt. *Sustain. Cities Soc.* **2019**, *47*, 101469. [CrossRef]
- Balu, N.J.; Lauby, M.G.; Kundur, P. *Power System Stability and Control*; Electrical Power Research Institute, McGraw-Hill Professional: Washington, DC, USA, 1994.
- Omer, A.M. Energy, environment and sustainable development. *Renew. Sustain. Energy Rev.* **2008**, *12*, 2265–2300. [CrossRef]
- Bilgen, S.; Kaygusuz, K.; Sari, A. Renewable Energy for a Clean and Sustainable Future. *Energy Sources* **2004**, *26*, 1119–1129. [CrossRef]
- Blaabjerg, F.; Teodorescu, R.; Liserre, M.; Timbus, A. Overview of Control and Grid Synchronization for Distributed Power Generation Systems. *IEEE Trans. Ind. Electron.* **2006**, *53*, 1398–1409. [CrossRef]
- Fang, J.; Li, H.; Tang, Y.; Blaabjerg, F. Distributed Power System Virtual Inertia Implemented by Grid-Connected Power Converters. *IEEE Trans. Power Electron.* **2017**, *33*, 8488–8499. [CrossRef]
- Bevrani, H. *Robust Power System Frequency Control*; Springer: Berlin/Heidelberg, Germany, 2009.
- Shahalami, S.H.; Farsi, D. Analysis of Load Frequency Control in a restructured multi-area power system with the Kalman filter and the LQR controller. *AEU-Int. J. Electron. Commun.* **2018**, *86*, 25–46. [CrossRef]
- Das, S.K.; Rahman, M.; Paul, S.K.; Armin, M.; Roy, P.N.; Paul, N. High-Performance Robust Controller Design of Plug-In Hybrid Electric Vehicle for Frequency Regulation of Smart Grid Using Linear Matrix Inequality Approach. *IEEE Access* **2019**, *7*, 116911–116924. [CrossRef]
- Liao, K.; Xu, Y. A Robust Load Frequency Control Scheme for Power Systems Based on Second-Order Sliding Mode and Extended Disturbance Observer. *IEEE Trans. Ind. Inform.* **2018**, *14*, 3076–3086. [CrossRef]
- HBevrani, H.; Feizi, M.R.; Atee, S. Robust Frequency Control in an Islanded Microgrid:  $H_\infty$  and  $\mu$ -Synthesis Approaches. *IEEE Trans. Smart Grid* **2015**, *7*, 706–717. [CrossRef]
- Wang, Z.-Q.; Sznaiar, M. Robust control design for load frequency control using  $\mu$ -synthesis. In Proceedings of the SOUTHCON'94, Orlando, FL, USA, 29–31 March 1994; pp. 186–190.
- Wang, Y.; Zhou, R.; Gao, L. H/sub  $\infty$ /controller design for power system load frequency control. In Proceedings of the TENCON'93, IEEE Region 10 International Conference on Computers, Communications and Automation, Beijing, China, 19–21 October 1993.
- Ma, M.; Liu, X.; Zhang, C. LFC for multi-area interconnected power system concerning wind turbines based on DMPC. *IET Gener. Transm. Distrib.* **2017**, *11*, 2689–2696. [CrossRef]

15. Khooban, M.H.; Gheisarnejad, M. A Novel Deep Reinforcement Learning Controller Based Type-II Fuzzy System: Frequency Regulation in Microgrids. *IEEE Trans. Emerg. Top. Comput. Intell.* **2021**, *5*, 689–699. [[CrossRef](#)]
16. Aluko, A.O.; Dorrell, D.G.; Pillay-Carpanen, R.; Ojo, E.E. Frequency Control of Modern Multi-Area Power Systems Using Fuzzy Logic Controller. In Proceedings of the 2019 IEEE PES/IAS PowerAfrica, Abuja, Nigeria, 20–23 August 2019.
17. Yang, D.; Jin, E.; You, J.; Hua, L. Dynamic Frequency Support from a DFIG-Based Wind Turbine Generator via Virtual Inertia Control. *Appl. Sci.* **2020**, *10*, 3376. [[CrossRef](#)]
18. Magdy, G.; Shabib, G.; Elbaset, A.A.; Mitani, Y. Renewable power systems dynamic security using a new coordination of frequency control strategy based on virtual synchronous generator and digital frequency protection. *Int. J. Electr. Power Energy Syst.* **2019**, *109*, 351–368. [[CrossRef](#)]
19. Mudi, R.K.; Pal, N.R. A self-tuning fuzzy PI controller. *Fuzzy Sets Syst.* **2000**, *115*, 327–338. [[CrossRef](#)]
20. Chang, C.; Fu, W. Area load frequency control using fuzzy gain scheduling of PI controllers. *Electr. Power Syst. Res.* **1997**, *42*, 145–152. [[CrossRef](#)]
21. Yesil, E.; Güzelkaya, M.; Eksin, I. Self tuning fuzzy PID type load and frequency controller. *Energy Convers. Manag.* **2004**, *45*, 377–390. [[CrossRef](#)]
22. Ahmadi, S.; Talami, S.H.; Sahnesaraie, M.A.; Dini, F.; Tahernejadjozam, B.; Ashgevari, Y. FUZZY aided PID controller is optimized by GA algorithm for Load Frequency Control of Multi-Source Power Systems. In Proceedings of the 2020 IEEE 18th World Symposium on Applied Machine Intelligence and Informatics (SAMII), Herlany, Slovakia, 23–25 January 2020.
23. Lal, D.K.; Barisal, A.K. Comparative performances evaluation of FACTS devices on AGC with diverse sources of energy generation and SMES. *Cogent Eng.* **2017**, *4*, 1318466. [[CrossRef](#)]
24. Lal, D.K.; Barisal, A.K.; Tripathy, M. Load Frequency Control of Multi Source Multi-Area Nonlinear Power System with DE-PSO Optimized Fuzzy PID Controller in Coordination with SSSC and RFB. *Int. J. Control. Autom.* **2018**, *11*, 61–80. [[CrossRef](#)]
25. Lal, D.K.; Barisal, A.K.; Tripathy, M. Load Frequency Control of Multi Area Interconnected Microgrid Power System using Grasshopper Optimization Algorithm Optimized Fuzzy PID Controller. In Proceedings of the 2018 Recent Advances on Engineering, Technology and Computational Sciences (RAETCS), Allahabad, India, 6–8 February 2018.
26. Dhanasekaran, B.; Siddhan, S.; Kaliannan, J. Ant colony optimization technique tuned controller for frequency regulation of single area nuclear power generating system. *Microprocess. Microsyst.* **2020**, *73*, 102953. [[CrossRef](#)]
27. Annamraju, A.; Nandiraju, S. Coordinated control of conventional power sources and PHEVs using jaya algorithm optimized PID controller for frequency control of a renewable penetrated power system. *Prot. Control. Mod. Power Syst.* **2019**, *4*, 28. [[CrossRef](#)]
28. Magdy, G.; Shabib, G.; Elbaset, A.A.; Kerdphol, T.; Qudaih, Y.; Mitani, Y. Decentralized optimal LFC for a real hybrid power system considering renewable energy sources. *J. Eng. Sci. Technol.* **2019**, *14*, 682–697.
29. Khamari, D.; Kumbhakar, B.; Patra, S.; Laxmi, D.A.; Panigrahi, S. Load Frequency Control of a Single Area Power System using Firefly Algorithm. *Int. J. Eng. Res.* **2020**, *V9*. [[CrossRef](#)]
30. Khadanga, R.K.; Kumar, A.; Panda, S. A hybrid shuffled frog-leaping and pattern search algorithm for load frequency controller design of a two-area system composing of PV grid and thermal generator. *Int. J. Numer. Model. Electron. Netw. Devices Fields* **2020**, *33*, e2694. [[CrossRef](#)]
31. Elkasem, A.H.A.; Kamel, S.; Rashad, A.; Jurado, F. Optimal Performance of DFIG Integrated with Different Power System Areas Using Multi-Objective Genetic Algorithm. In Proceedings of the 2018 Twentieth International Middle East Power Systems Conference (MEPCON), Cairo, Egypt, 18–20 December 2018; pp. 672–678.
32. Elkasem, A.H.A.; Kamel, S.; Korashy, A.; Nasrat, L. Load Frequency Control Design of Two Area Interconnected Power System Using GWO. In Proceedings of the 2019 IEEE Conference on Power Electronics and Renewable Energy (CPERE), Aswan, Egypt, 23–25 October 2019.
33. Kamel, S.; Elkasem, A.H.A.; Korashy, A.; Ahmed, M.H. Sine Cosine Algorithm for Load Frequency Control Design of Two Area Interconnected Power System with DFIG Based Wind Turbine. In Proceedings of the 2019 International Conference on Computer, Control, Electrical and Electronics Engineering (ICCCEEE), Khartoum, Sudan, 21–23 September 2019.
34. Hamdy, A.; Kamel, S.; Nasrat, L.; Jurado, F. Frequency Stability of Two-Area Interconnected Power System with Doubly Fed Induction Generator Based Wind Turbine. In *Wide Area Power Systems Stability, Protection, and Security*; Springer: Berlin/Heidelberg, Germany, 2021; pp. 293–324.
35. Khamies, M.; Magdy, G.; Hussein, M.E.; Banakhr, F.A.; Kamel, S. An Efficient Control Strategy for Enhancing Frequency Stability of Multi-Area Power System Considering High Wind Energy Penetration. *IEEE Access* **2020**, *8*, 140062–140078. [[CrossRef](#)]
36. Khamies, M.; Magdy, G.; Ebeed, M.; Kamel, S. A robust PID controller based on linear quadratic gaussian approach for improving frequency stability of power systems considering renewables. *ISA Trans.* **2021**, *117*, 118–138. [[CrossRef](#)] [[PubMed](#)]
37. Gürses, D.; Bureerat, S.; Sait, S.M.; Yildiz, A.R. Comparison of the arithmetic optimization algorithm, the slime mold optimization algorithm, the marine predators algorithm, the salp swarm algorithm for real-world engineering applications. *Mater. Test.* **2021**, *63*, 448–452. [[CrossRef](#)]
38. Abualigah, L.; Diabat, A.; Sumari, P.; Gandomi, A. A Novel Evolutionary Arithmetic Optimization Algorithm for Multilevel Thresholding Segmentation of COVID-19 CT Images. *Processes* **2021**, *9*, 1155. [[CrossRef](#)]
39. Dash, P.; Saikia, L.C.; Sinha, N. Flower Pollination Algorithm Optimized PI-PD Cascade Controller in Automatic Generation Control of a Multi-area Power System. *Int. J. Electr. Power Energy Syst.* **2016**, *82*, 19–28. [[CrossRef](#)]

40. Guha, D.; Roy, P.; Banerjee, S. Load frequency control of interconnected power system using grey wolf optimization. *Swarm Evol. Comput.* **2016**, *27*, 97–115. [[CrossRef](#)]
41. Ibraheem; Nizamuddin; Bhatti, T.S. AGC of two area power system interconnected by AC/DC links with diverse sources in each area. *Int. J. Electr. Power Energy Syst.* **2014**, *55*, 297–304. [[CrossRef](#)]
42. Neshat, M.; Nezhad, M.M.; Abbasnejad, E.; Mirjalili, S.; Tjernberg, L.B.; Garcia, D.A.; Alexander, B.; Wagner, M. A deep learning-based evolutionary model for short-term wind speed forecasting. *Energy Convers. Manag.* **2021**, *236*, 114002. [[CrossRef](#)]
43. Li, D.; Jiang, F.; Chen, M.; Qian, T. Multi-step-ahead wind speed forecasting based on a hybrid decomposition method and temporal convolutional networks. *Energy* **2022**, *238*, 121981. [[CrossRef](#)]
44. Emeksiz, C.; Tan, M. Multi-step wind speed forecasting and Hurst analysis using novel hybrid secondary decomposition approach. *Energy* **2022**, *238*, 121764. [[CrossRef](#)]
45. Jiang, P.; Liu, Z.; Niu, X.; Zhang, L. A combined forecasting system based on statistical method, artificial neural networks, and deep learning methods for short-term wind speed forecasting. *Energy* **2021**, *217*, 119361. [[CrossRef](#)]
46. Deveci, M.; Özcan, E.; John, R.; Pamucar, D.; Karaman, H. Offshore wind farm site selection using interval rough numbers based Best-Worst Method and MARCOS. *Appl. Soft Comput.* **2021**, *109*, 107532. [[CrossRef](#)]
47. Deveci, M.; Erdogan, N.; Cali, U.; Stekli, J.; Zhong, S. Type-2 neutrosophic number based multi-attributive border approximation area comparison (MABAC) approach for offshore wind farm site selection in USA. *Eng. Appl. Artif. Intell.* **2021**, *103*, 104311. [[CrossRef](#)]
48. Jena, T.; Debnath, M.K.; Sanyal, S.K. Optimal fuzzy-PID controller with derivative filter for load frequency control including UPFC and SMES. *IJECE* **2019**, *9*, 2813. [[CrossRef](#)]
49. Mohanty, B.; Panda, S.; Hota, P.K. Controller parameters tuning of differential evolution algorithm and its application to load frequency control of multi-source power system. *Int. J. Electr. Power Energy Syst.* **2014**, *54*, 77–85. [[CrossRef](#)]
50. Sahu, B.K.; Pati, T.K.; Nayak, J.R.; Panda, S.; Kar, S.K. A novel hybrid LUS–TLBO optimized fuzzy-PID controller for load frequency control of multi-source power system. *Int. J. Electr. Power Energy Syst.* **2016**, *74*, 58–69. [[CrossRef](#)]
51. Parmar, K.S.; Majhi, S.; Kothari, D. Load frequency control of a realistic power system with multi-source power generation. *Int. J. Electr. Power Energy Syst.* **2012**, *42*, 426–433. [[CrossRef](#)]
52. Magdy, G.; Mohamed, E.A.; Shabib, G.; Elbaset, A.A.; Mitani, Y. SMES based a new PID controller for frequency stability of a real hybrid power system considering high wind power penetration. *IET Renew. Power Gener.* **2018**, *12*, 1304–1313. [[CrossRef](#)]
53. Kickert, W.; Lemke, H.V.N. Application of a fuzzy controller in a warm water plant. *Automatica* **1976**, *12*, 301–308. [[CrossRef](#)]
54. Sahu, B.K.; Pati, S.; Panda, S. Hybrid differential evolution particle swarm optimisation optimised fuzzy proportional–integral derivative controller for automatic generation control of interconnected power system. *IET Gener. Transm. Distrib.* **2014**, *8*, 1789–1800. [[CrossRef](#)]
55. Zangeneh, M.; Aghajari, E.; Forouzanfar, M. A survey: Fuzzify parameters and membership function in electrical applications. *Int. J. Dyn. Control* **2020**, *8*, 1040–1051. [[CrossRef](#)]
56. Sadollah, A. Introductory Chapter: Which Membership Function is Appropriate in Fuzzy System? In *Fuzzy Logic Based in Optimization Methods and Control Systems and its Applications*; InTech Open: Rijeka, Croatia, 2018.
57. Abualigah, L.; Diabat, A.; Mirjalili, S.; Elaziz, M.A.; Gandomi, A.H. The Arithmetic Optimization Algorithm. *Comput. Methods Appl. Mech. Eng.* **2021**, *376*, 113609. [[CrossRef](#)]